Optical Properties of Atmospheric Aerosols

Russell Philbrick[a,b] and Hans Hallen[a]
[a]Physics Department, [b]Marine Earth and Atmospheric Sciences Department
NC State University, Raleigh NC 27695-8202

36th Review of Atmospheric Transmission Models (ATM) Conference
9-11 June 2015 at the Hotel Hyatt Dulles in Herndon, VA

Physical Processes Governing Transmission Through Aerosols

(1) Aerosol Size Compared with Wavelength

As size increases, the cross-section $\sigma \sim r^6$ for $\lambda < r$, and $\sigma \sim r^2$ for $\lambda > r$, where r is a spherical particle radius. The relative scattering cross-section at two wavelengths depends on (frequency ratio)^4, i.e. $(\nu_2/\nu_1)^4$, or $(\lambda_1/\lambda_2)^4$.

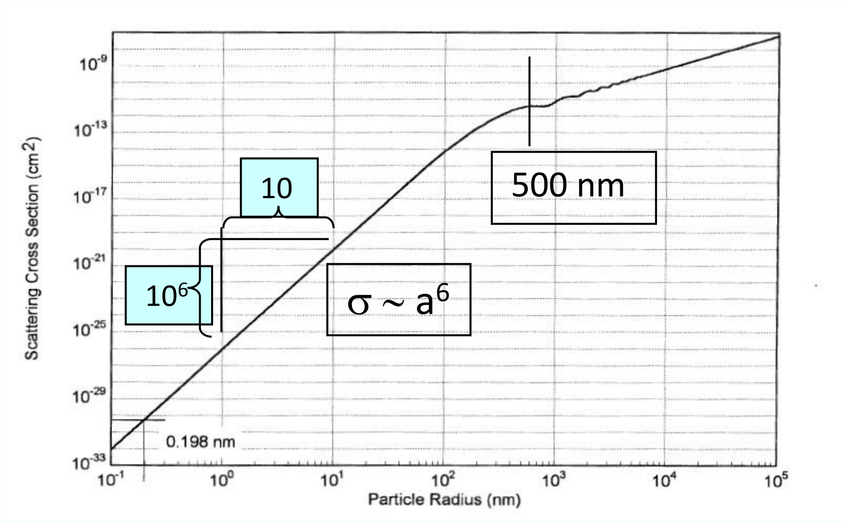

Scattering cross section of dielectric sphere:

$$\sigma = 4\pi[(\varepsilon - \varepsilon_o)/\varepsilon + 2\varepsilon_o)]^2 k^4 a^6 \sin^2\theta$$

Backscatter cross section:

$$\sigma_{back} \sim a^6$$

(2) Aerosol Shape Complicates Transmission Road/Agriculture/Desert Dust

Scattering from water vapor and other liquid aerosols can be easily described and scattering phase functions are useful in describing the size distribution. Irregular shape aerosols require more complex analysis and some knowledge of the typical size and composition to analyze.

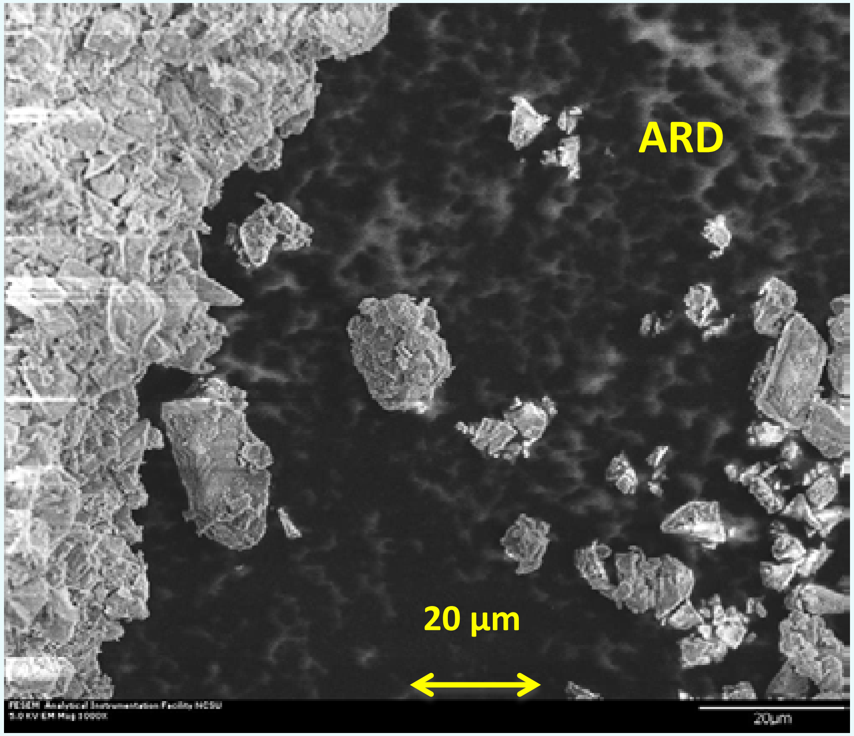

Physical Processes Governing Transmission Through Aerosols

(3) Aerosol Complex Index of Refraction

The chemical makeup of an aerosol strongly influences the transmission. The real component of the index governs the scattering and the imaginary component describes the absorption. An additional factor that can complicate the transmission calculation is the thickness of the material, which can hide part of the aerosol's effect if the material is optically thick at a wavelength of interest.

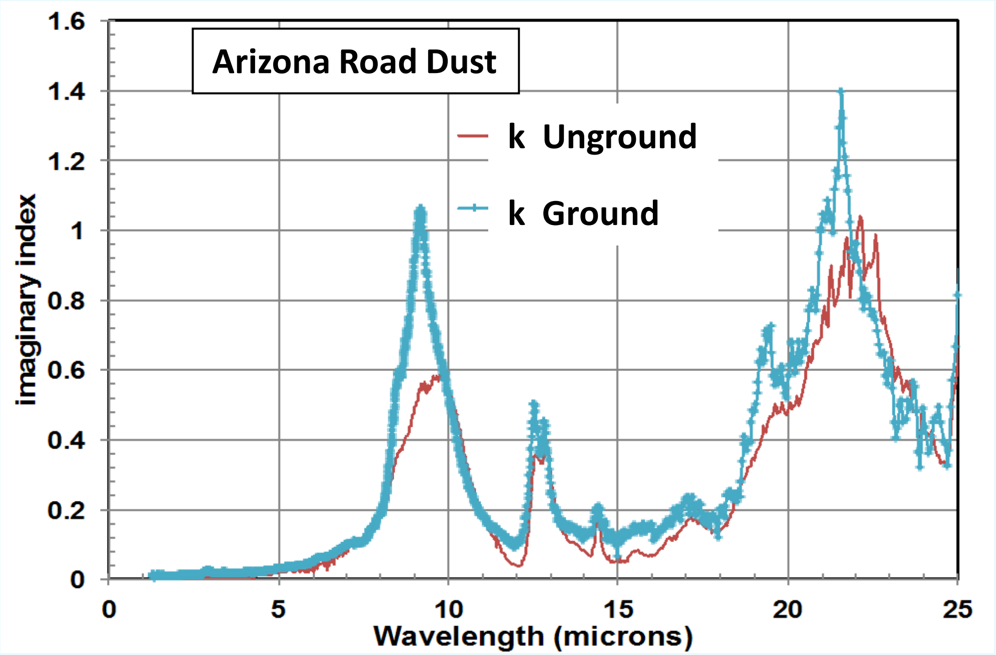

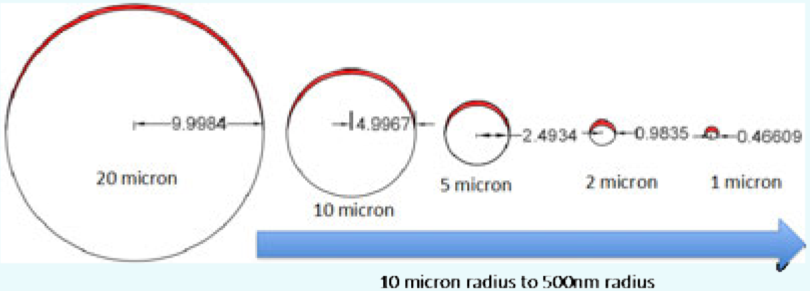

(4)The Spatial Distribution of Aerosols Describes Transmission

The many ways that aerosols are generated results in complex patterns and residence time are influenced by wind, diffusion, settling time, and chemical processes.

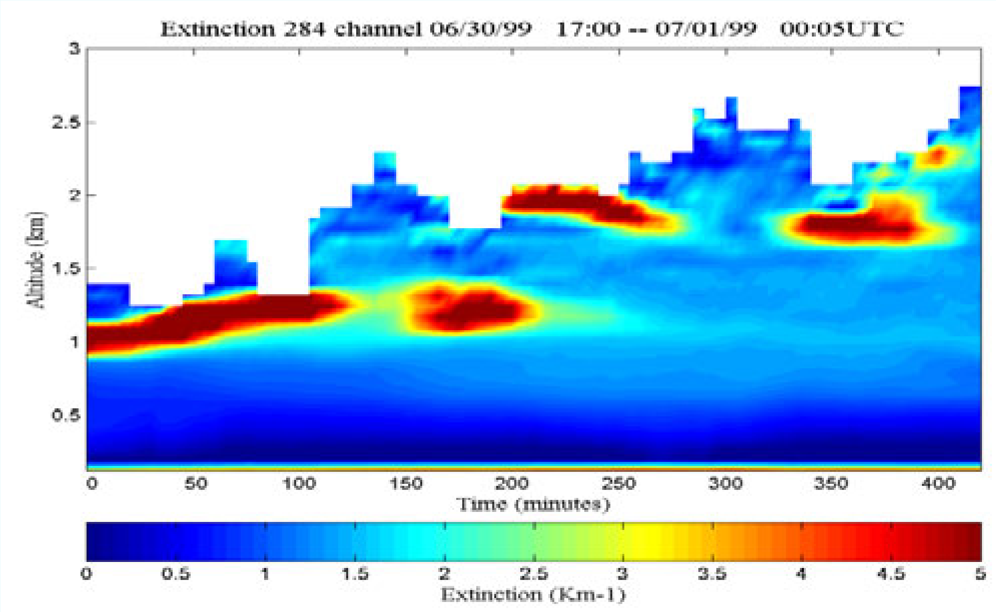

Raman Lidar Provides an Important Tool for Extinction Profiles

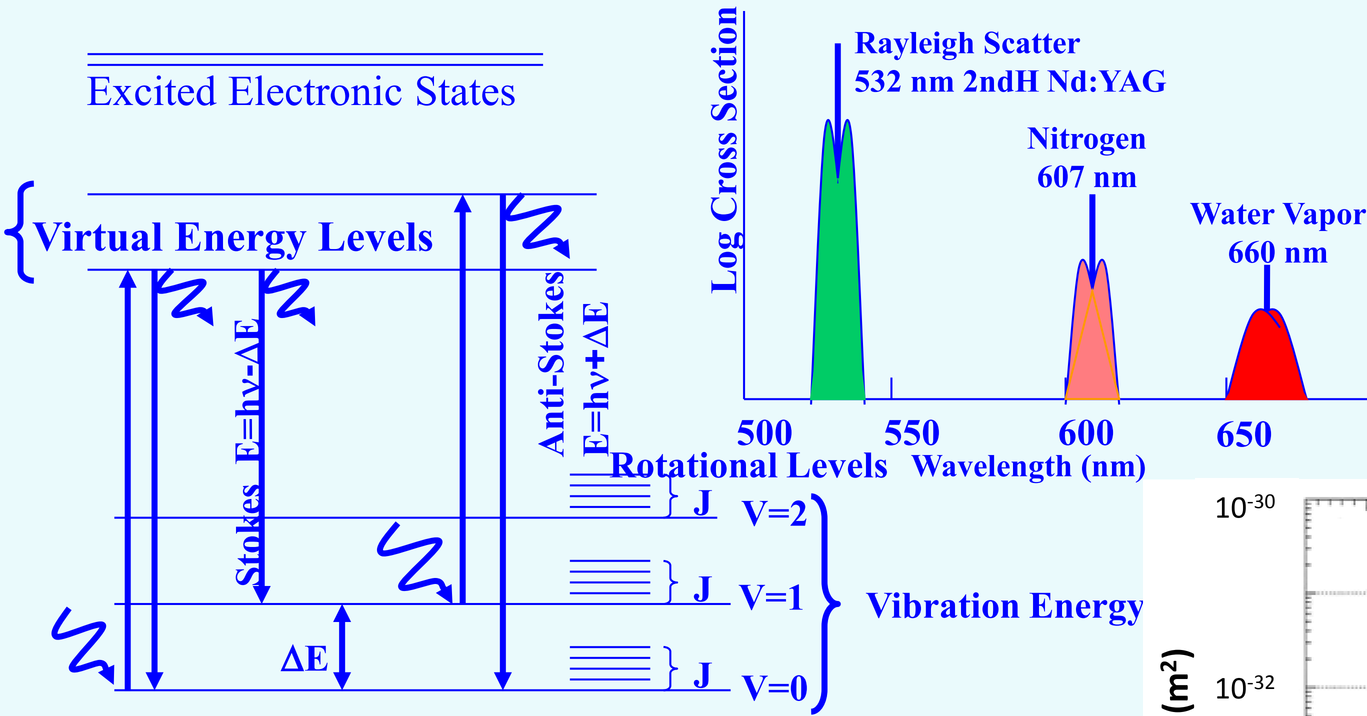

Rotational Raman, ΔJ states, are distributed by the thermal energy and describe the local temperature.

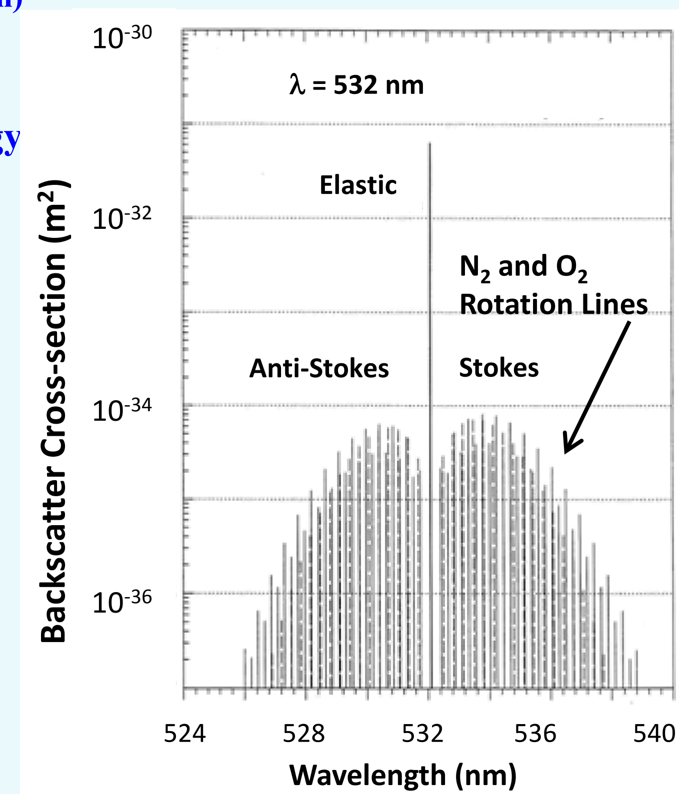

Vibrational Raman transitions to Virtual Energy level relaxes to a unique vibrational level of the molecule. Concentrations the major molecules in the atmosphere, N_2, O_2, H_2O, O_3, CO_2, … , can be determined relative to N_2 using their Raman signal and laboratory measured cross-section.

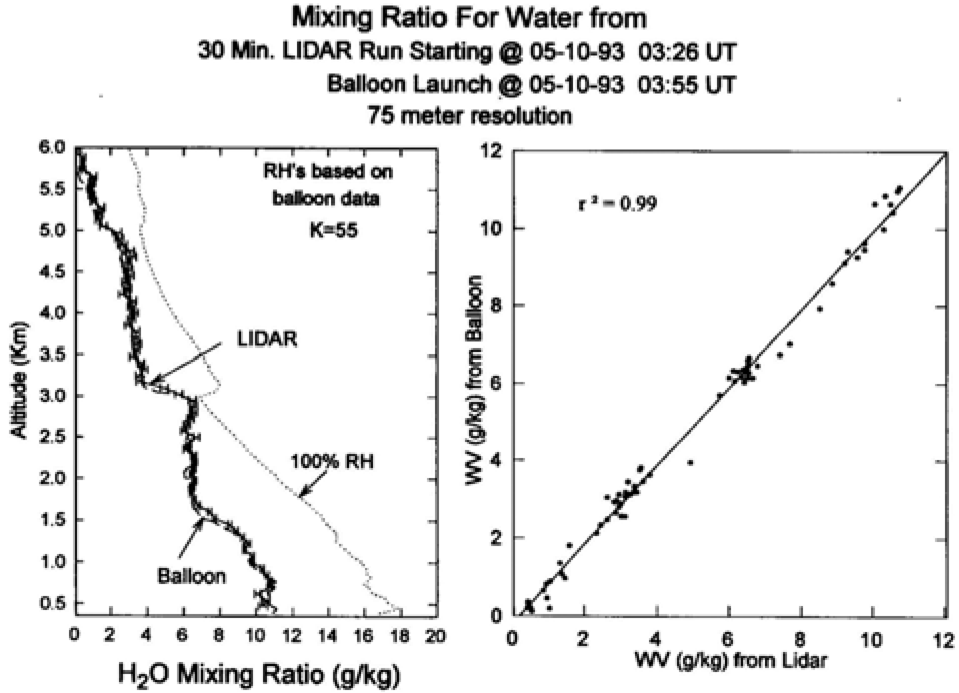

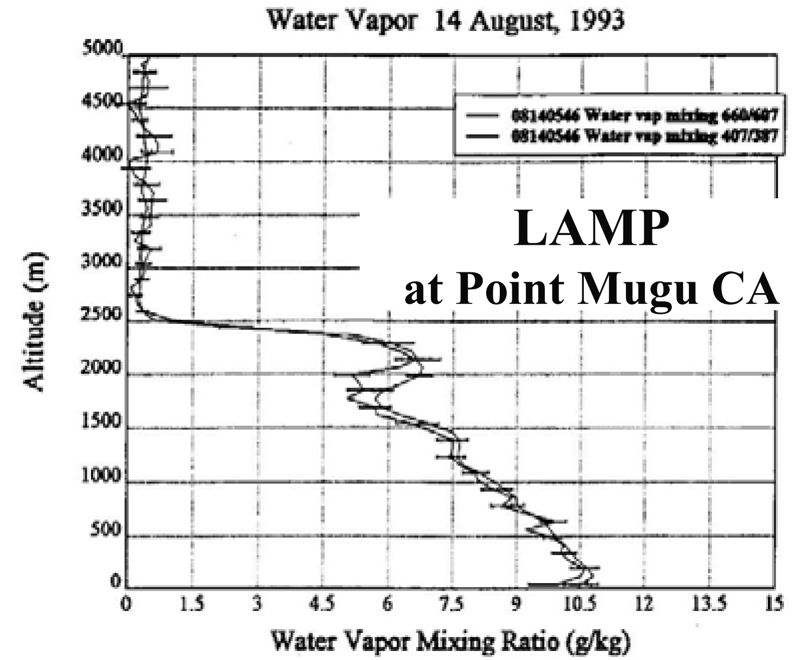

LAMP at Point Mugu CA

Raman Lidar for Water Vapor and Temperature

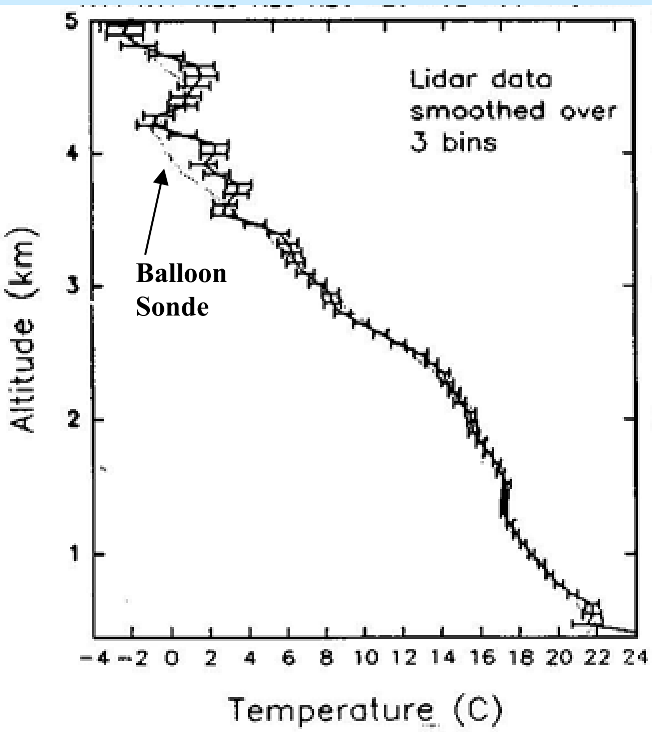

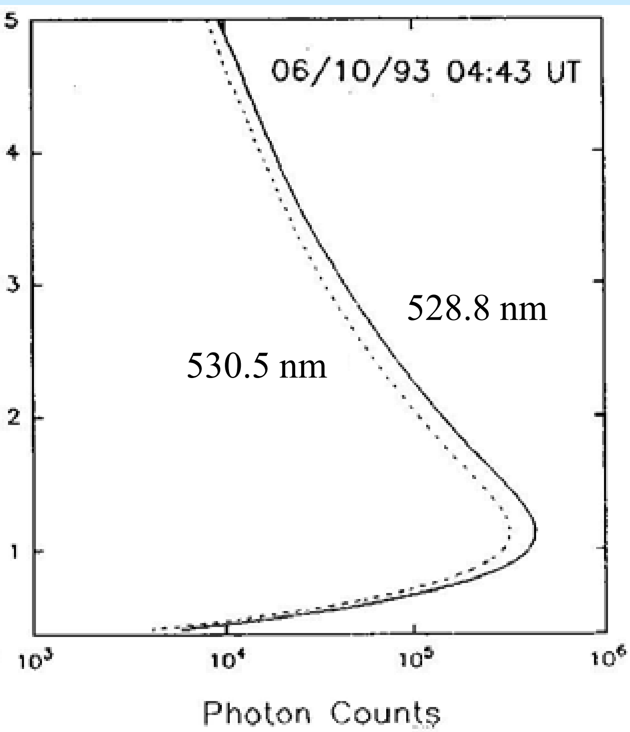

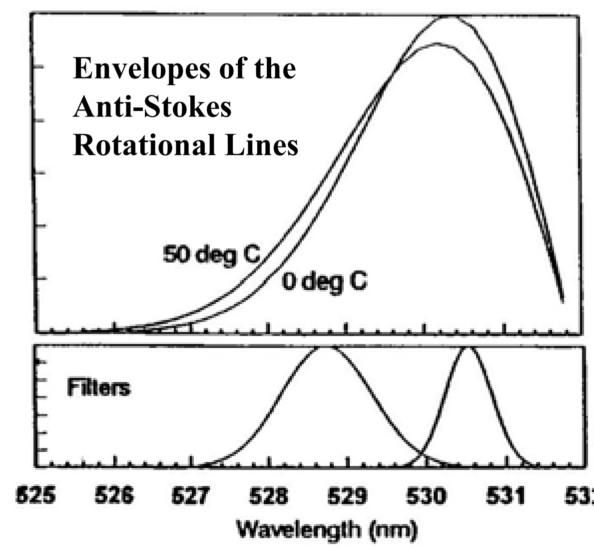

Raman Lidar Optical Extinction

$$I = I_0\, e^{-\alpha z}$$

Signal intensity (corrected for $1/z^2$) will follow hydrostatic profile in a pure molecular atmosphere without scattering loss – the difference from that molecular profile gradient is extinction.

$$\alpha_{tot} = \alpha_{mol\ scat} + \alpha_{aer\ scat} + \alpha_{mol\ abs} + \alpha_{aer\ abs}$$

$$\alpha_R^{aer} = \frac{d}{dz}\left[\ln \frac{N_R(z)}{P_R(z)\cdot z^2}\right] - \alpha_{scat}^{mol}(z) - \alpha_{abs}^{mol}(z) - \alpha_{abs}^{aer}(z)$$

$$\alpha_{532}^{aer} = \frac{d}{dz}\left[\frac{1}{2}\ln \frac{N(z)}{P_{530}(z)\cdot z^2}\right] - \alpha_{532}^{mol}(z) \quad .$$

O - outgoing – 532, 355, or 266 nm

R - return - 530 (rot), 607 (N_2), 285 (N_2) or 276 (O_2) nm

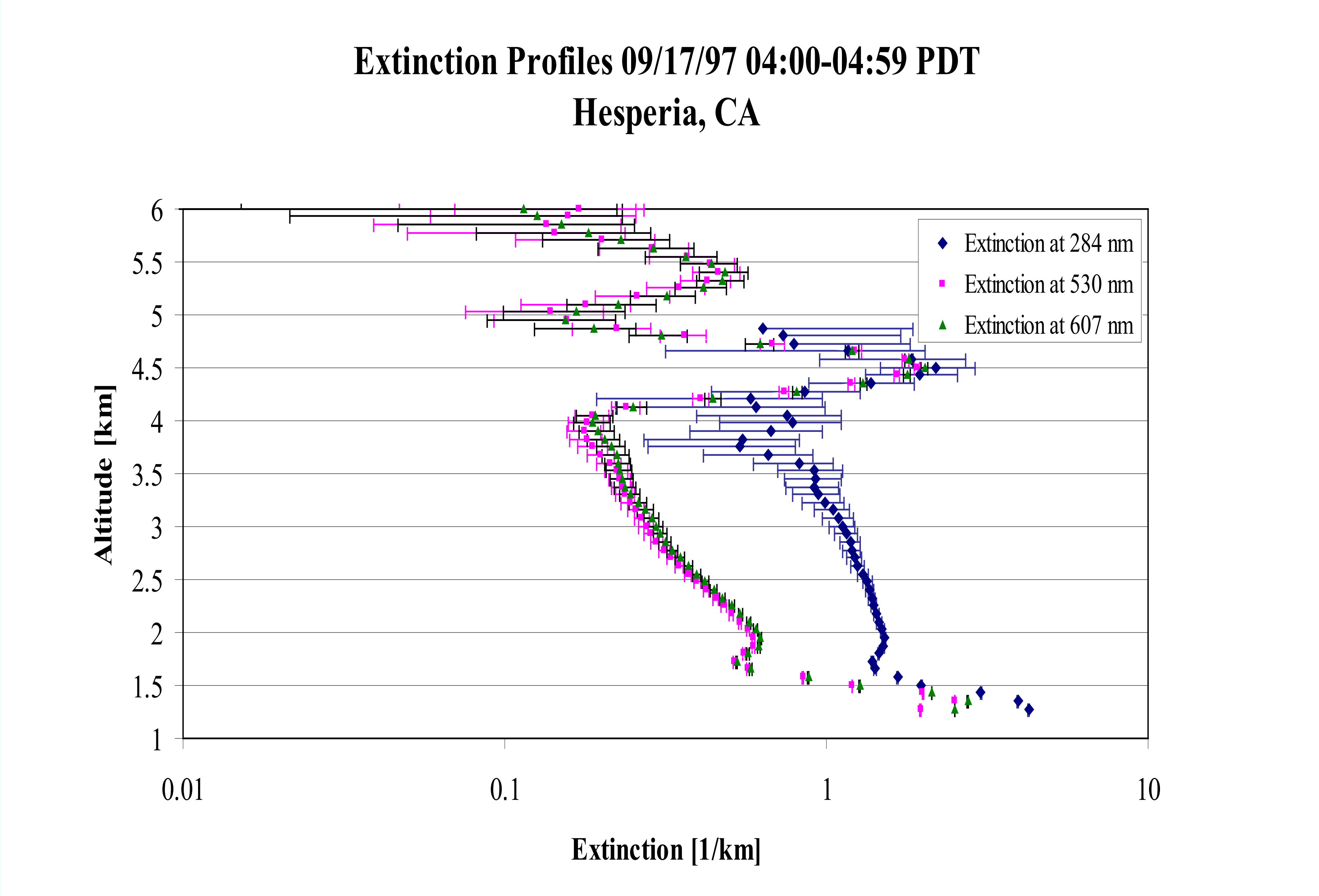

The multi-wavelength lidar profiles show a larger number of smaller aerosol particles present over most of the height, but when a cloud is encountered near 4 km, all of the wavelengths indicate the same extinction due to multiple scattering.

Time sequence and integrated profiles of optical extinction – SCOS 97

The lidar data is typically gathered in 1-min integrated profiles that are stacked side-by-side and then a 5-min smoothing filter is applied.

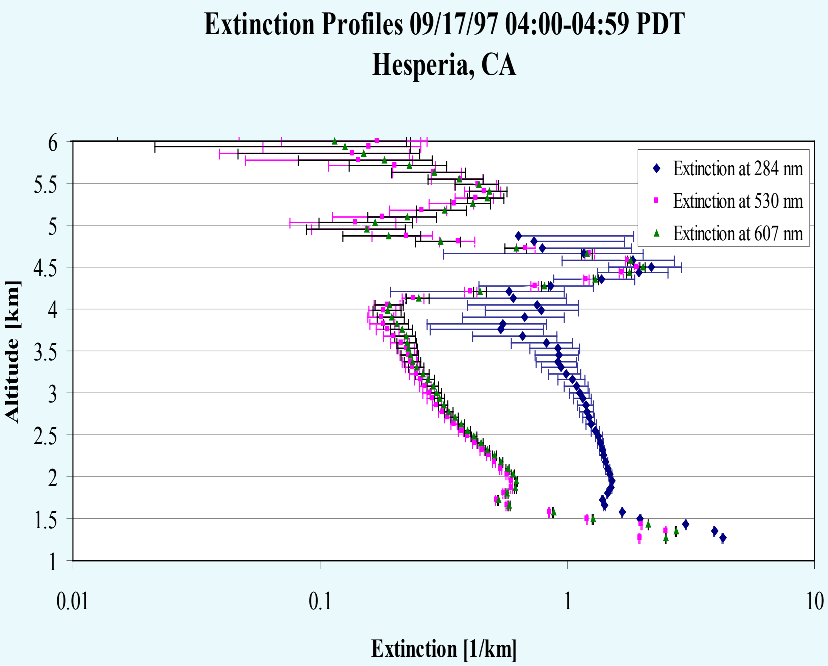

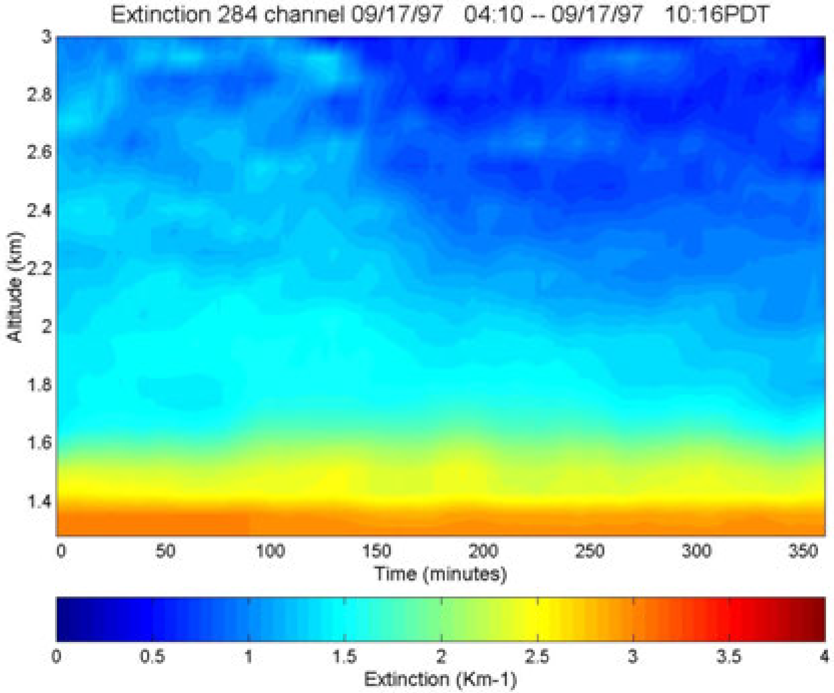

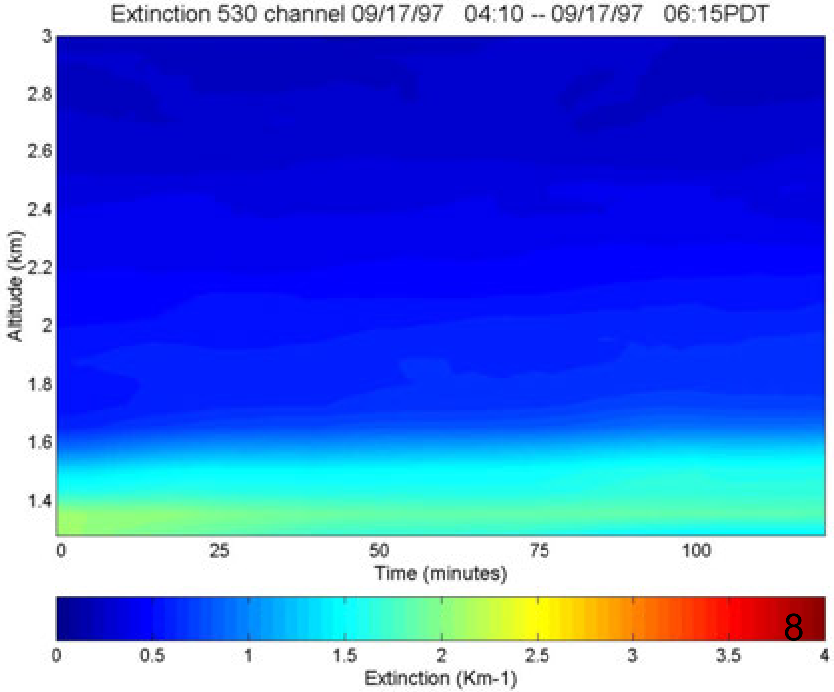

The Raman Lidar thus allows us to study the troposphere in the same way that we could by releasing an instrumented weather balloon every few minutes each day.

A quick view of the next few slides show some of the important ways that Raman Lidar now contributes to our knowledge of the atmosphere. These examples include the following cases:
(1-2) The night before a major air pollution event, we see a moist layer moving into the area and then being rapidly transported to the ground by encounter with the rising morning convective boundary layer. A back-trajectory calculation shows that it came from the Ohio Valley, and EPA measurements at the site show it contains the chemical, PAN, which is a power plant emission. The PAN quickly dissociates and forms smog aerosols as shown in the extinction plot.
(3) The relation of PM2.5 and PM10 (EPA surface sensors) correlated to lidar extinction at 800 m (lidar measurement in the mixed PBL 24 hr).
(4) A surface measurement shows the strong correlation of extinction with water vapor.
(5-6) Opportunities to use Raman Lidar to study cloud micro-physics are shown.

NARSTO-NE-OPS 1998
Transport Initiated Pollution Event -
PAN from Ohio Valley Power Plants

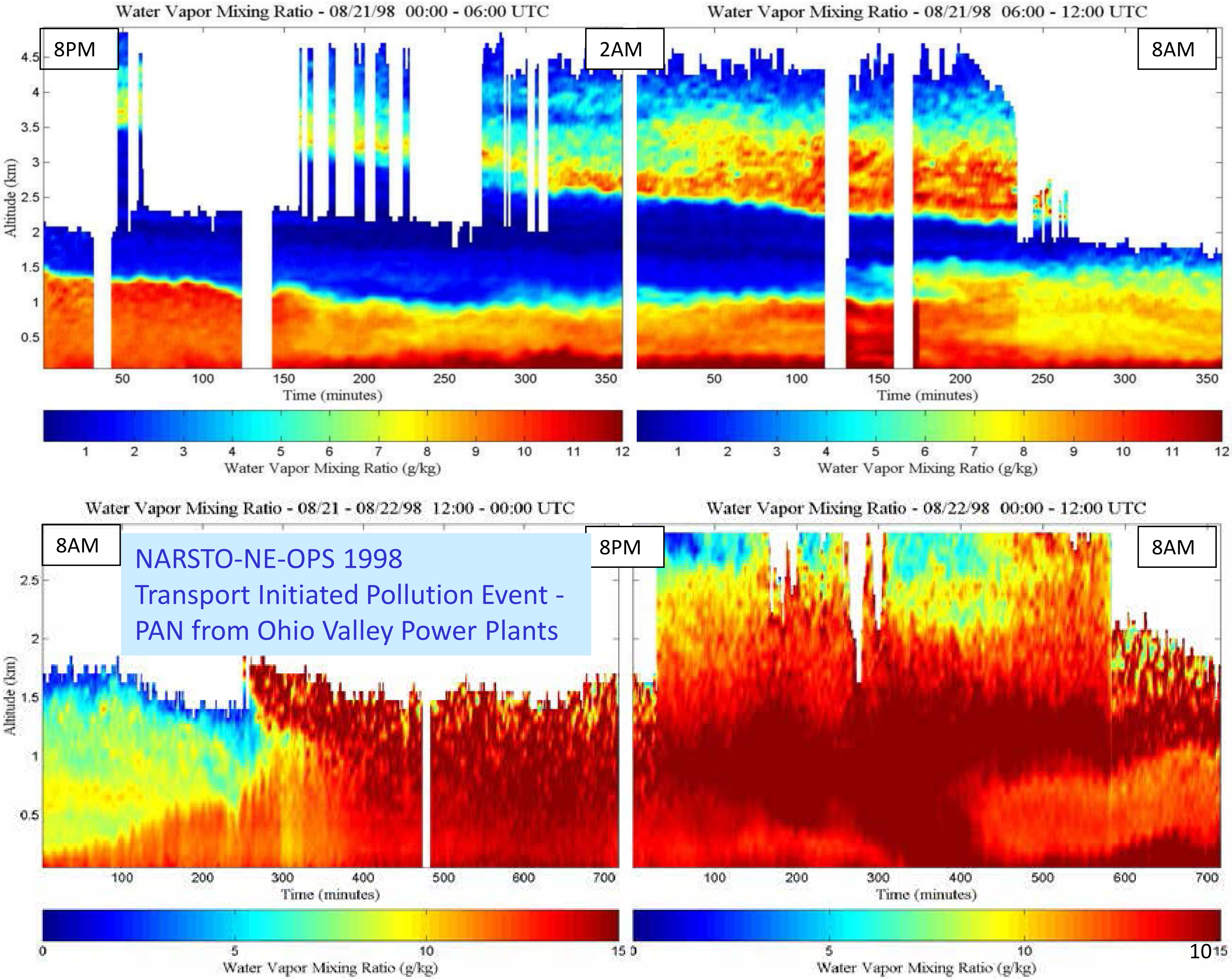

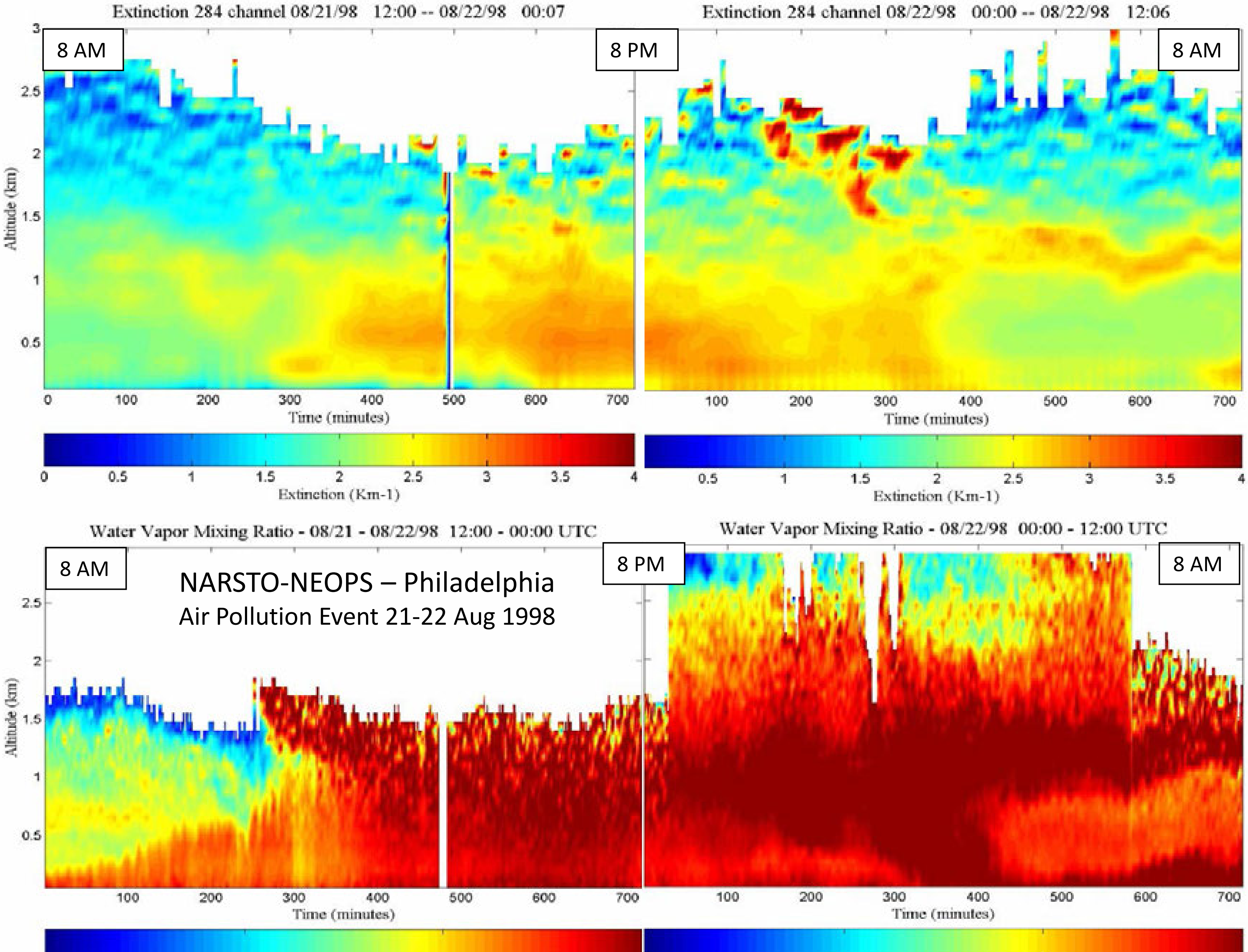
Extinction 284 channel 08/21/98 12:00 -- 08/22/98 00:07
Extinction 284 channel 08/22/98 00:00 -- 08/22/98 12:06
8 AM
8 PM
8 AM
Altitude (km)
Time (minutes)
Extinction (Km-1)
Water Vapor Mixing Ratio - 08/21 - 08/22/98 12:00 - 00:00 UTC
Water Vapor Mixing Ratio - 08/22/98 00:00 - 12:00 UTC
8 AM
8 PM
8 AM
NARSTO-NEOPS – Philadelphia
Air Pollution Event 21-22 Aug 1998
Altitude (km)
Time (minutes)
Water Vapor Mixing Ratio (g/kg)

Lidar Optical Extinction Compared to PM_{10} and $PM_{2.5}$

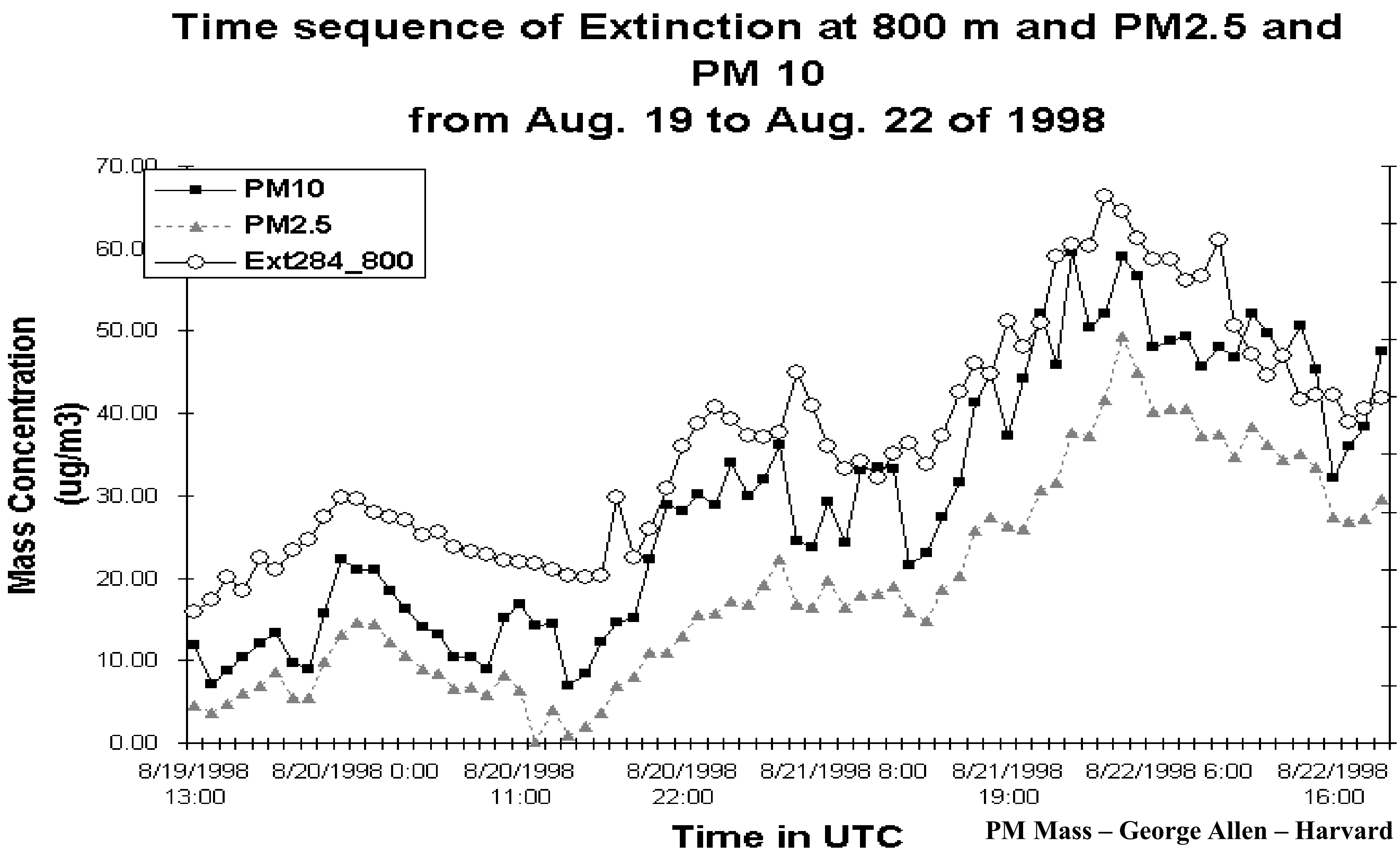

PM Mass – George Allen – Harvard SPH

Humidity control of extinction

>80% relative humidity causes striking increase in small particle extinction
(primarily due to drop in nighttime temperature)

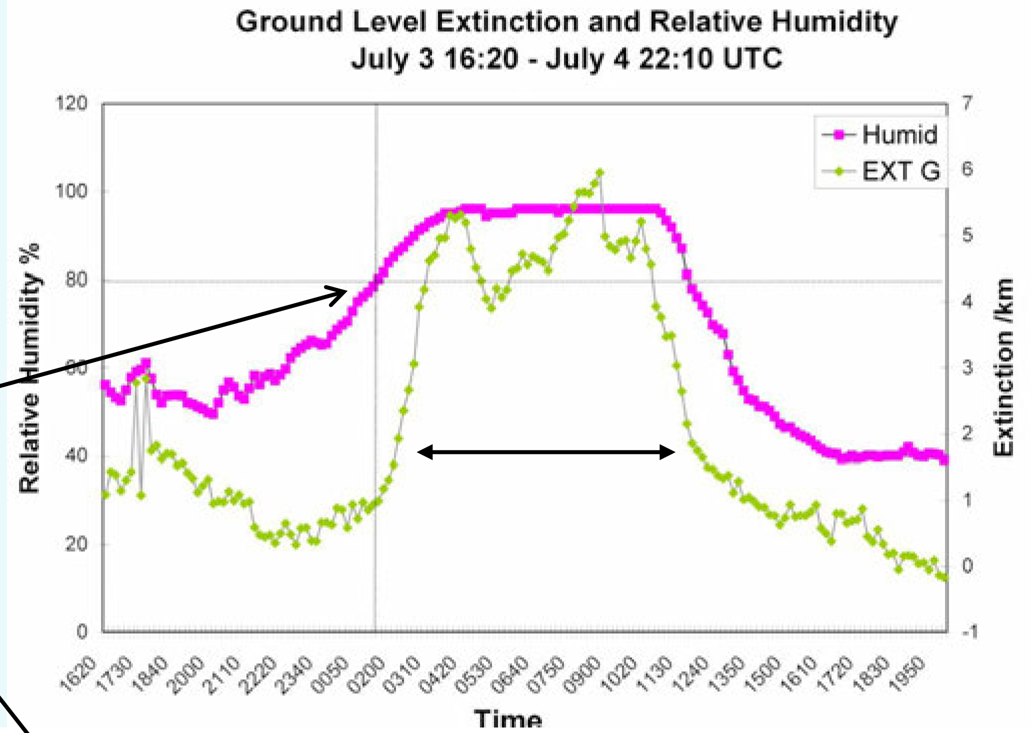

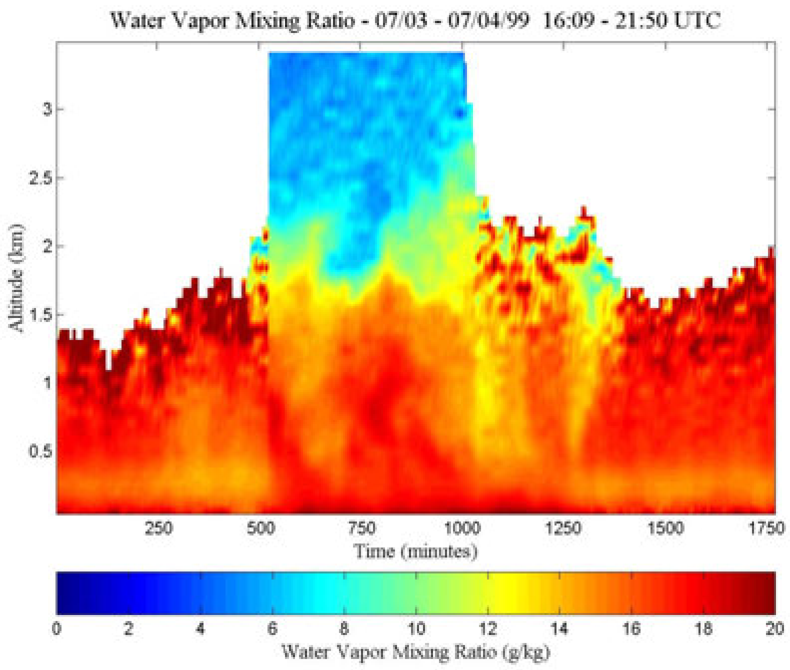

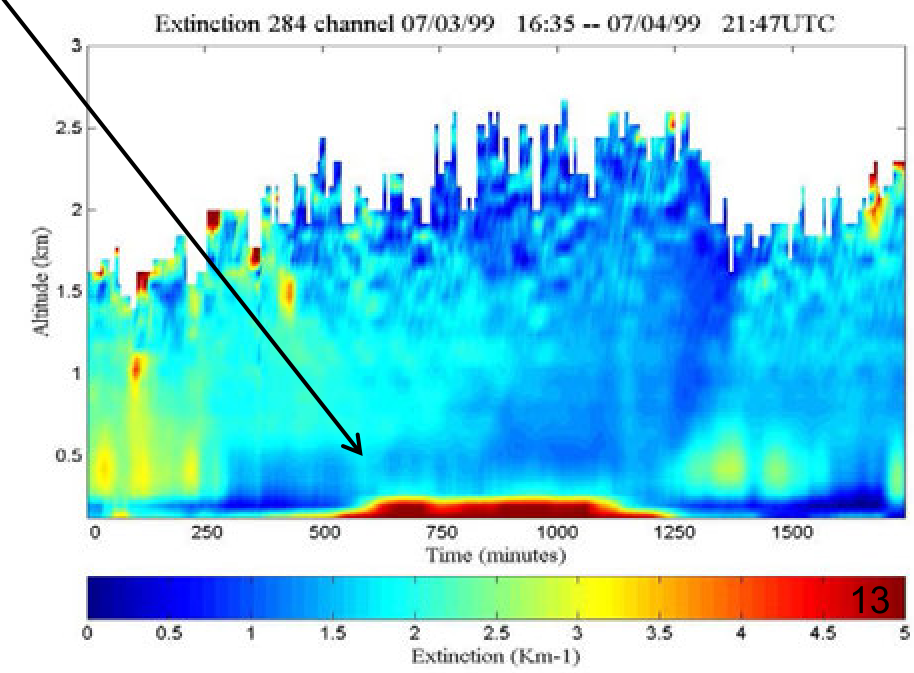

Scattering from Cloud

Cloud scattering at visible and ultraviolet wavelengths -

- multi-λ to infer size variation
- SH in region around cloud indicates growth or dissipation

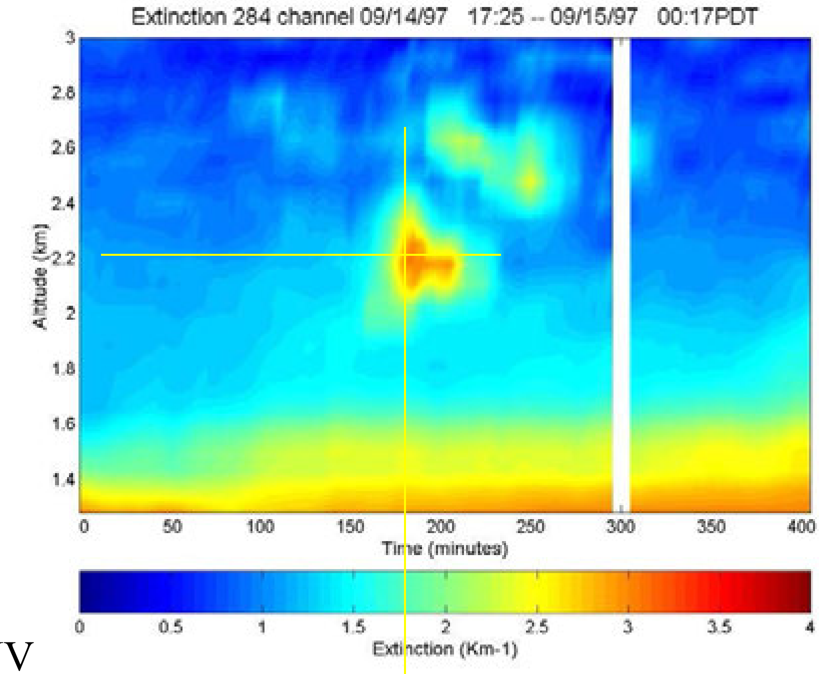

UV

VIS | H_2O

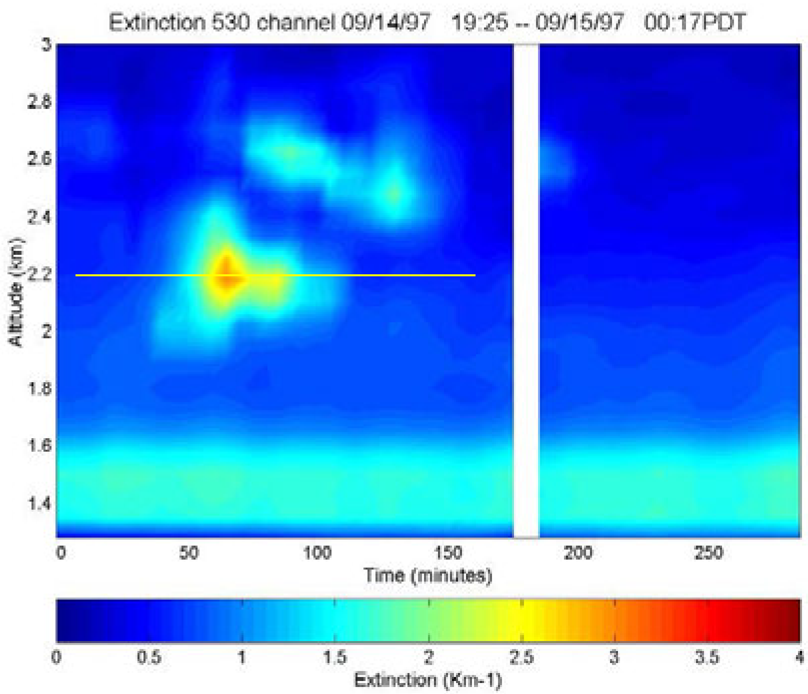

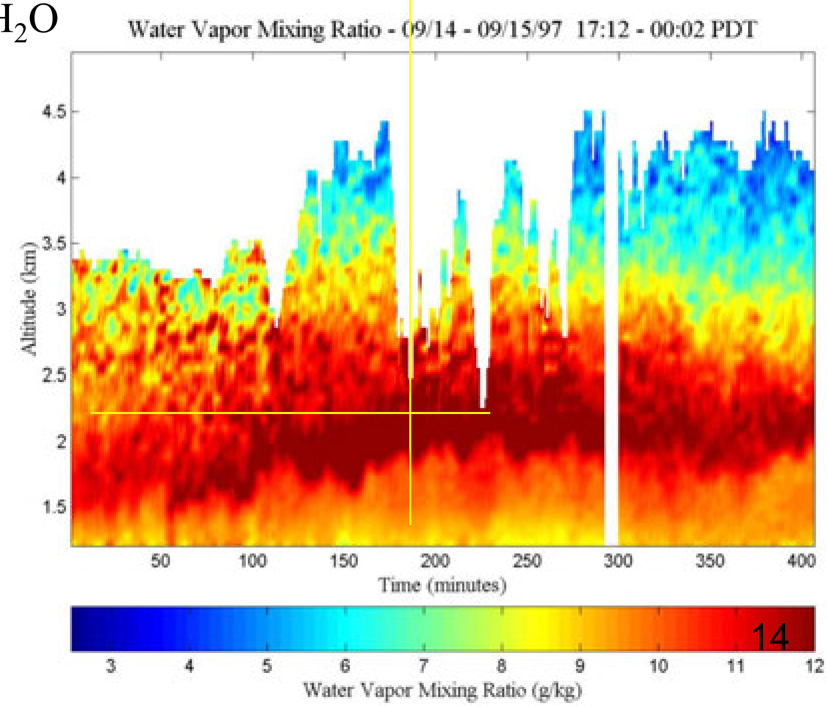

The time sequence shows the evolution of a cloud in terms of the local water vapor content and small particle extinction.

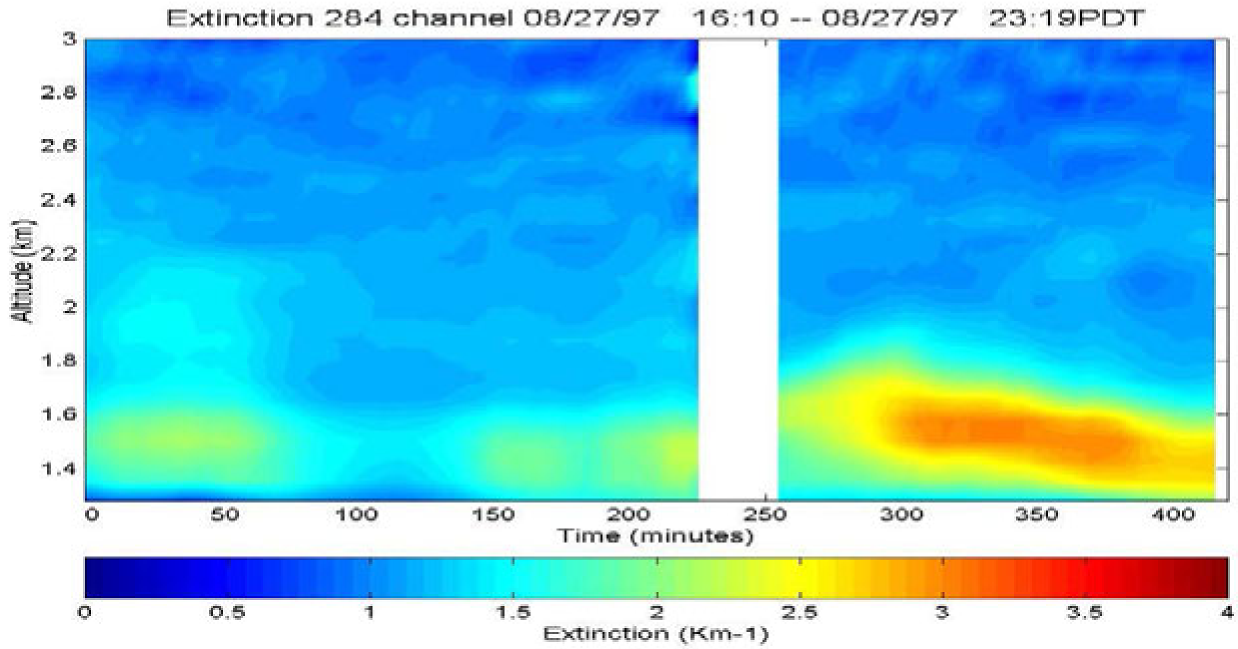

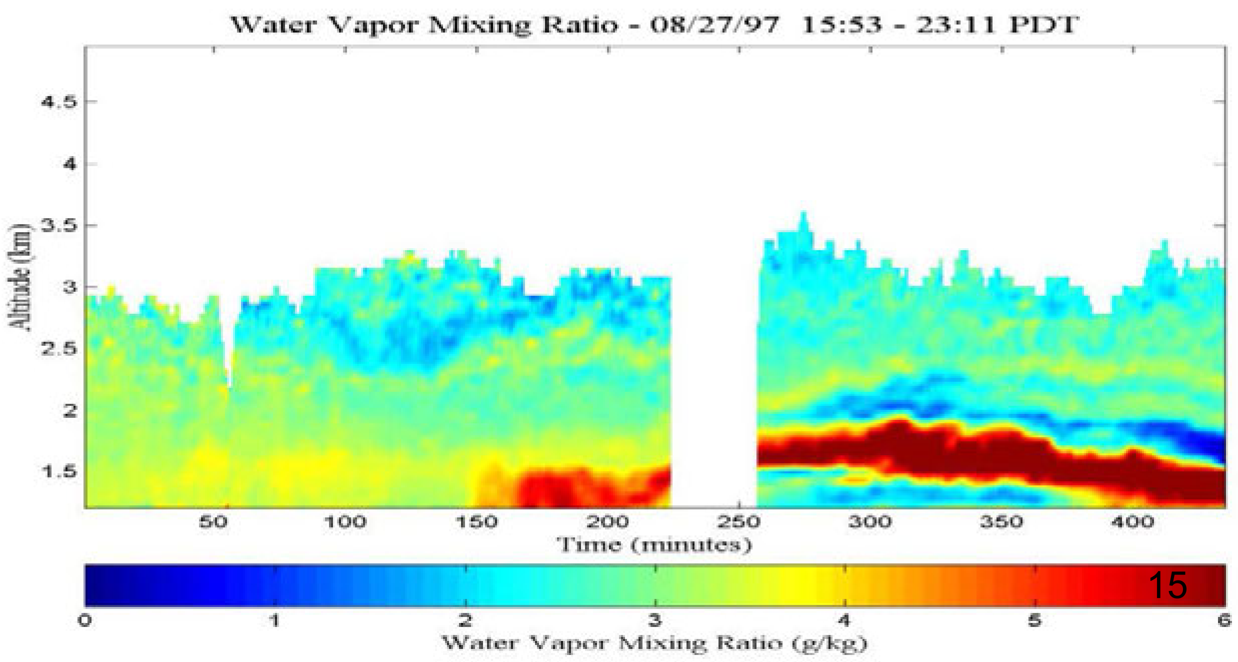

Using the N_2, O_2 and the rotational signals from Raman Lidar, we are able to measure the path optical extinction at UV, VIS, NIR wavelengths near the laser wavelength we choose, but we must avoid wavelengths where chemical absorption occurs (high values of k). Most of the visible and near ultraviolet region has sufficiently low absorption, due to peaks in the imaginary index of refraction, that the Raman lidar technique provides excellent profiles of optical extinction. However, we often need to better understand the optical path in the presence of aerosols composed of various absorbing chemicals, and those particles that are in condensed and irregular forms, such as airborne dusts.

In solid materials, the optical scatter process is complicated by internal electric fields from nearby charge distributions. Effective medium theory is used to better describe these more complicated environments and extend measurements into the infrared region, where absorption features dominate. The use of ellipsometry, infrared absorption measurements, and electron microscopy, together with development of sample preparation techniques, now provide an opportunity to characterize these complex optical environments.

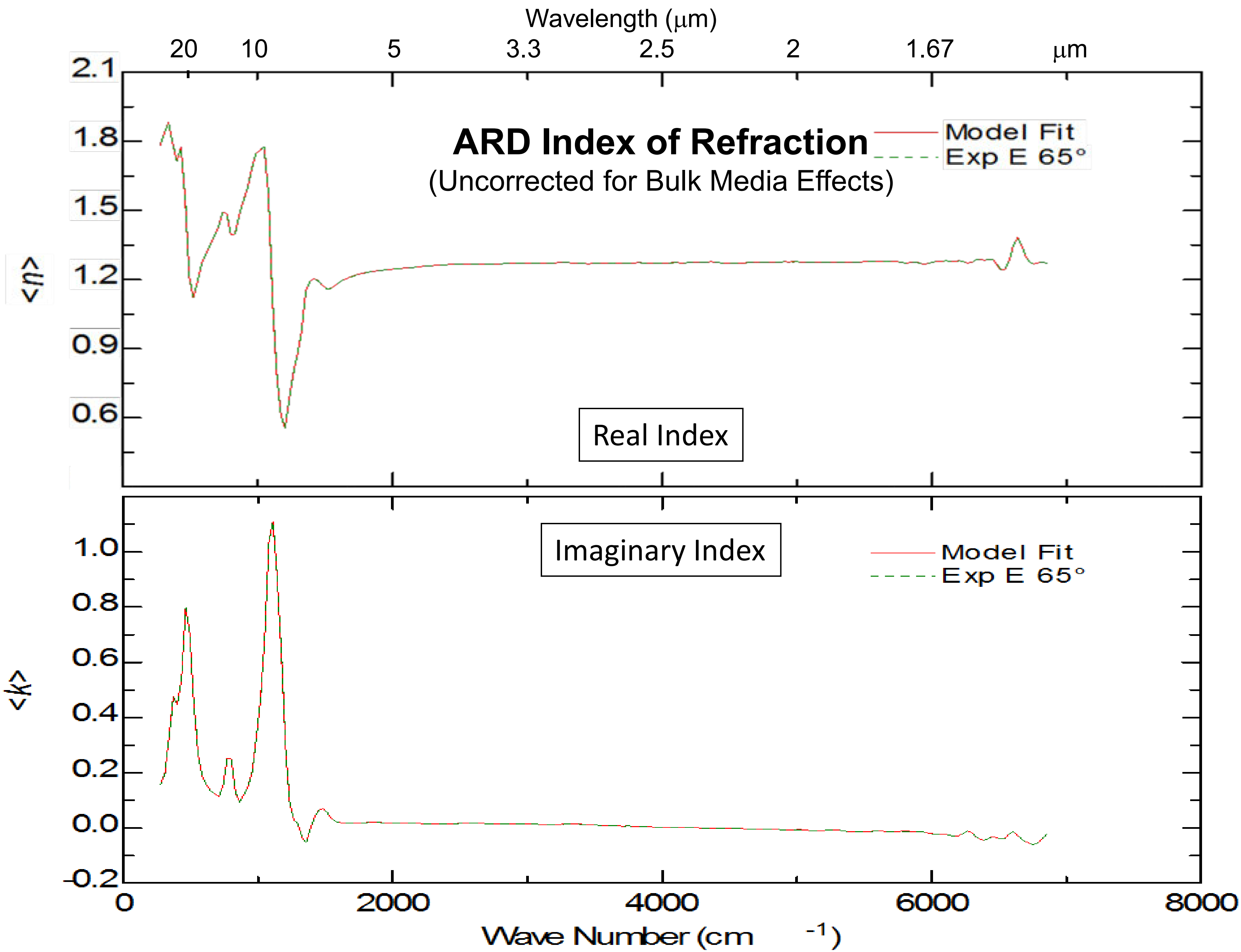
Wavelength (μm)
20
10
5
3.3
2.5
2
1.67
μm
ARD Index of Refraction
(Uncorrected for Bulk Media Effects)
Model Fit
Exp E 65°
Real Index
<n>
2.1
1.8
1.5
1.2
0.9
0.6
Imaginary Index
Model Fit
Exp E 65°
<k>
1.0
0.8
0.6
0.4
0.2
0.0
-0.2
0
2000
4000
6000
8000
Wave Number (cm -1)

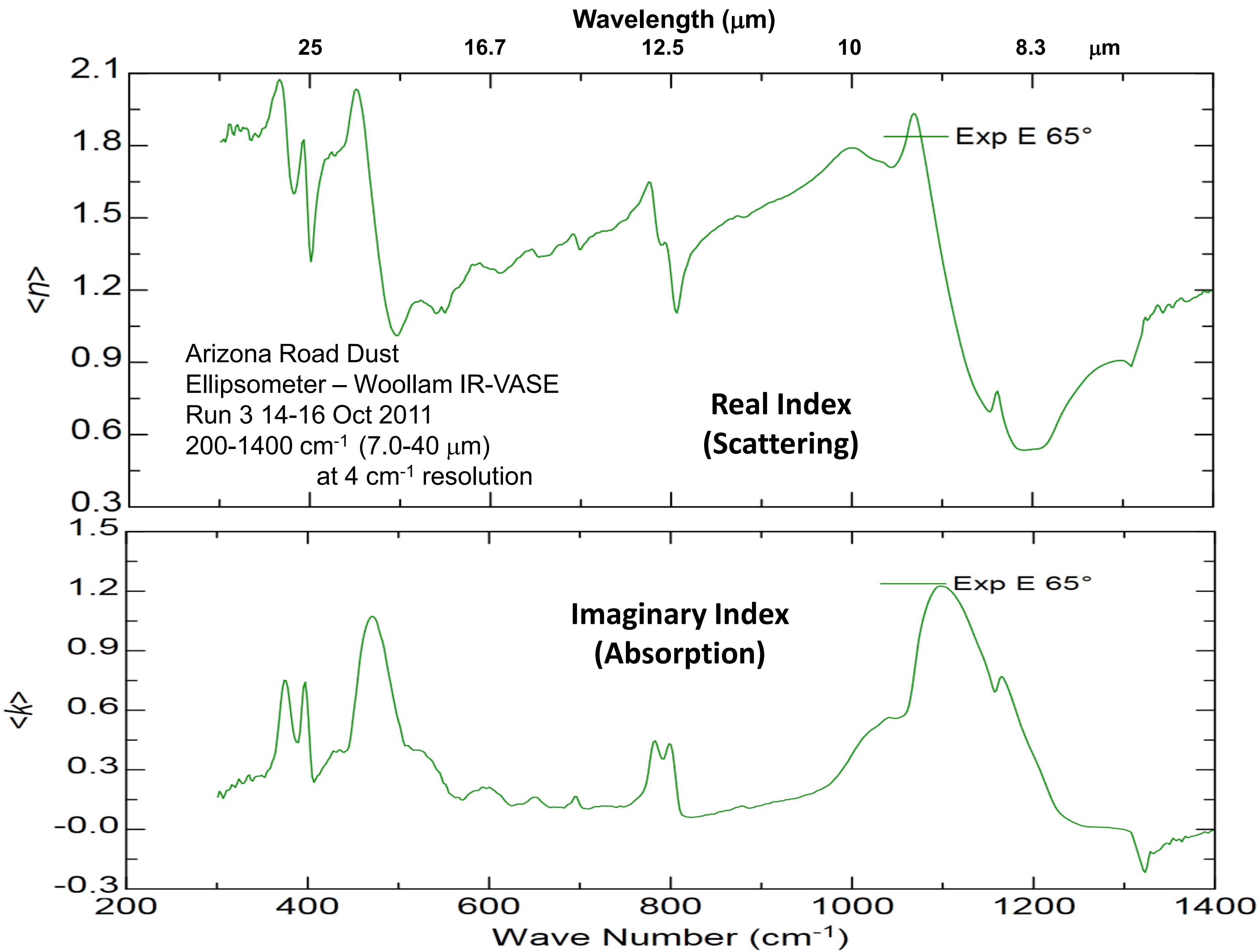

Wavelength (μm)
25
16.7
12.5
10
8.3
μm
2.1
1.8
1.5
1.2
0.9
0.6
0.3
<n>
Exp E 65°
Arizona Road Dust
Ellipsometer – Woollam IR-VASE
Run 3 14-16 Oct 2011
200-1400 cm-1 (7.0-40 μm)
at 4 cm-1 resolution
Real Index
(Scattering)
1.5
1.2
0.9
0.6
0.3
-0.0
-0.3
<k>
Exp E 65°
Imaginary Index
(Absorption)
200
400
600
800
1000
1200
1400
Wave Number (cm-1)

Ellipsometry Measurements of the Real and Imaginary Index
Arizona Road Dust (ARD)

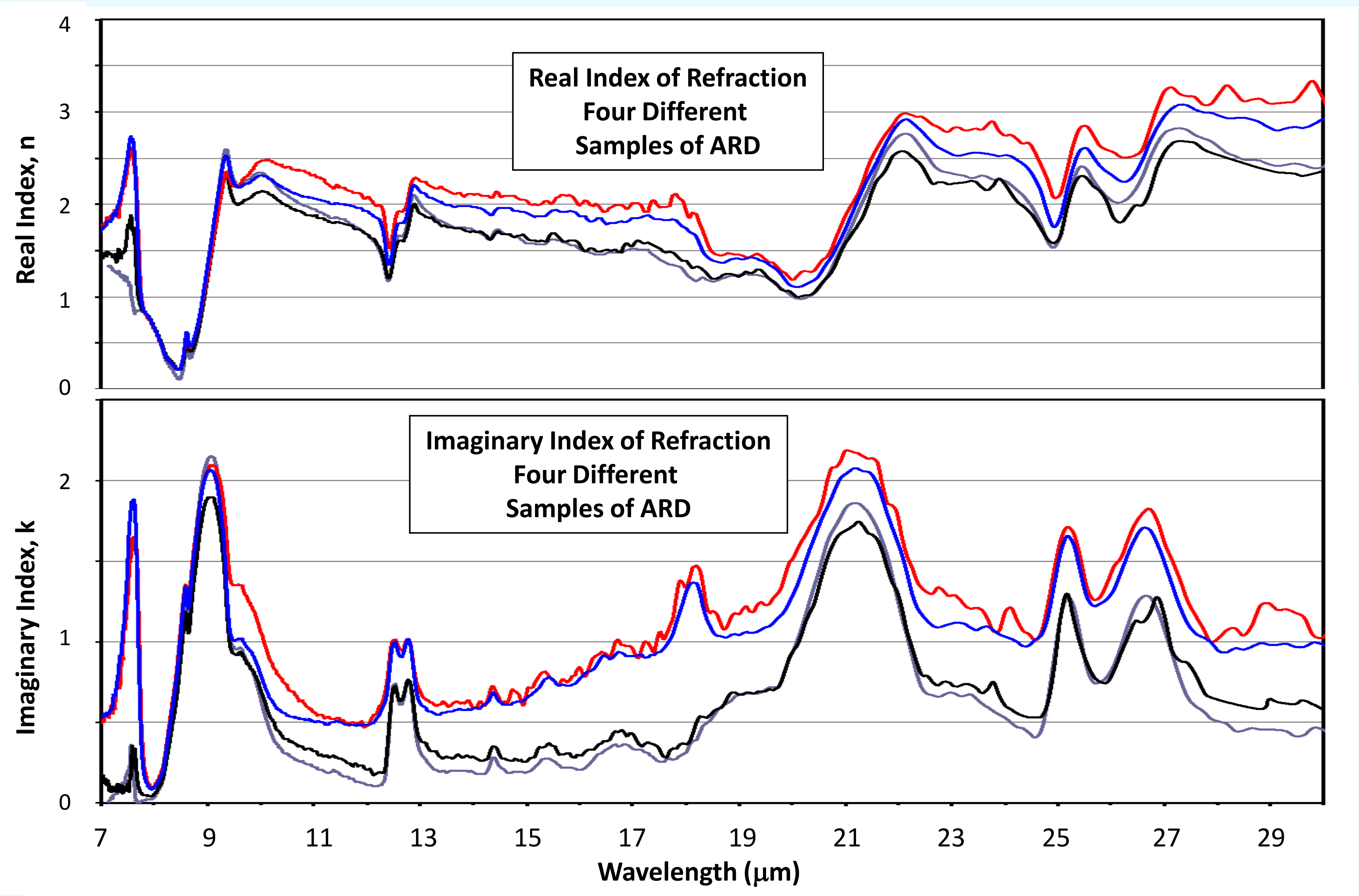

Correction of the Index

- The index is obviously wrong for something mostly silica.
- Mix silica (~1.5) and air (~1) and get something in between.
- Solution depends upon the geometry.
- Use the dielectric constant $\varepsilon = (n - ik)^2$

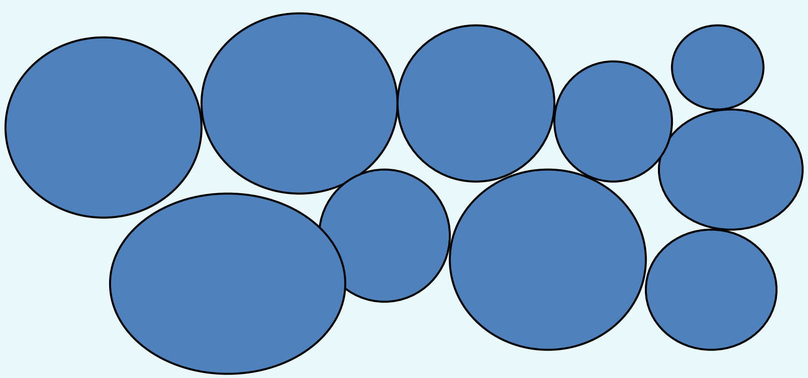

A warning about geometry

- Limiting cases are
  - No screening
    $$\varepsilon = f_a \varepsilon_a + f_b \varepsilon_b$$
  - Maximum screening
    $$\varepsilon = \left(f_a / \varepsilon_a + f_b / \varepsilon_b \right)^{-1}$$
- Capacitance works when << wavelength.
- The spheres case is in between.

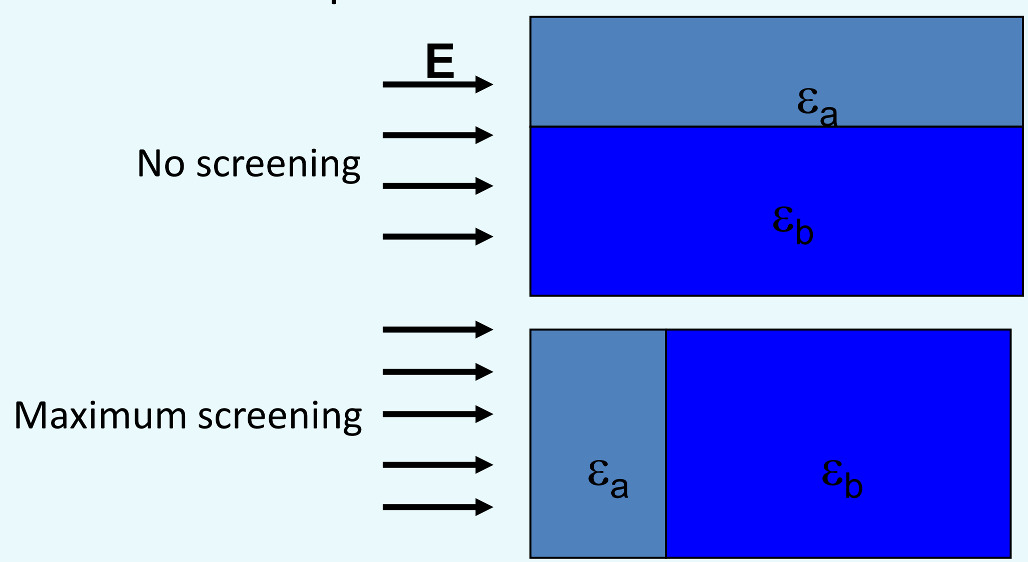

Effective Medium Theory

- Assumes that the granularity is small compared to the wavelength (λ/4).
- Models randomly placed spheres.
- Has been found to work well even over a broad wavelength range.

Aspnes, Am. J. Phys. **50**(8) 704, 1982; Phys.Rev. B**26**(10), 5313, 1982.

$$0 = f_a \frac{\varepsilon_a - \varepsilon}{\varepsilon_a + 2\varepsilon} + f_b \frac{\varepsilon_b - \varepsilon}{\varepsilon_b + 2\varepsilon}$$

- The f's are volume fractions.
- The dielectric constants are ε_a the dust dielectric constant, ε_b =1 for air, and ε the host dielectric constant , which is what the composite material will look like (if the assumptions hold).
- We measure ε and the volume fractions, only ε_a is unknown.
- There are corrections for larger particles.

Bistatic Methodology for Scattering Phase Function Information

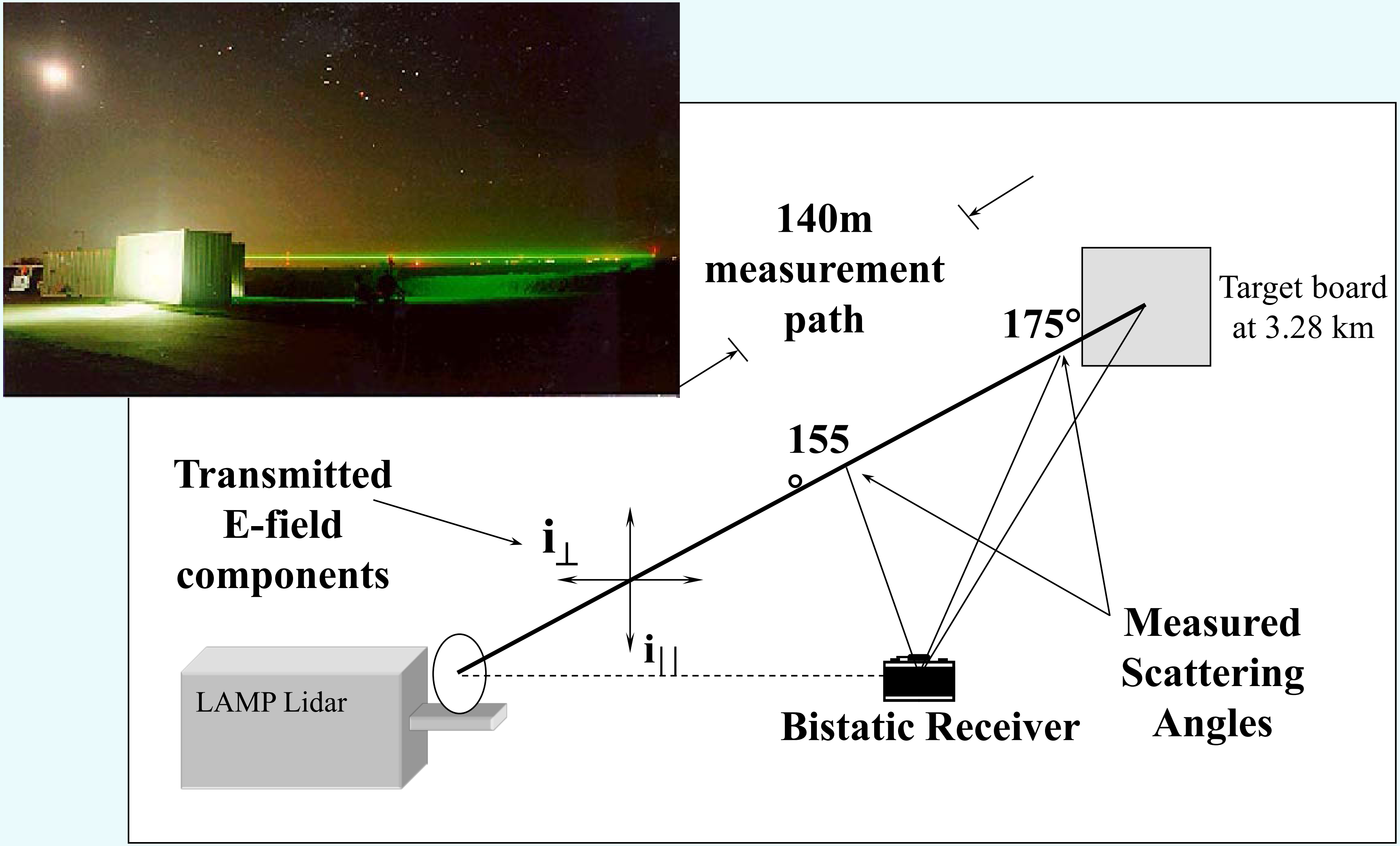

Scattering Phase Function & Polarization Ratio

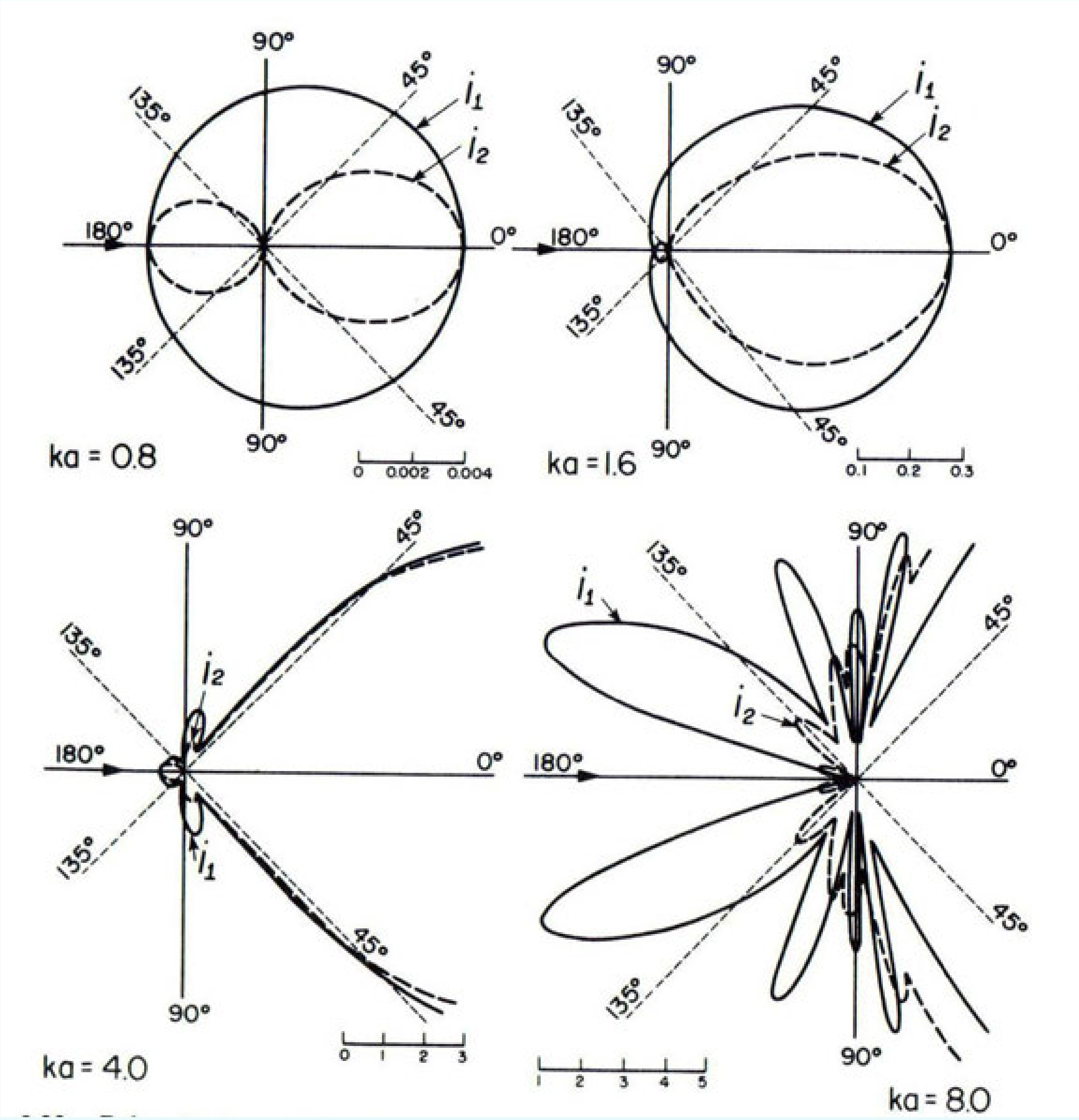

Backscatter –
Bistatic Lidar

Forward Lobe –
Aureole Laser

Born and Wolf,
Principals of Optics,
Cambridge Press 2002

Polarization Components of the Scattering Phase Function

10 μm

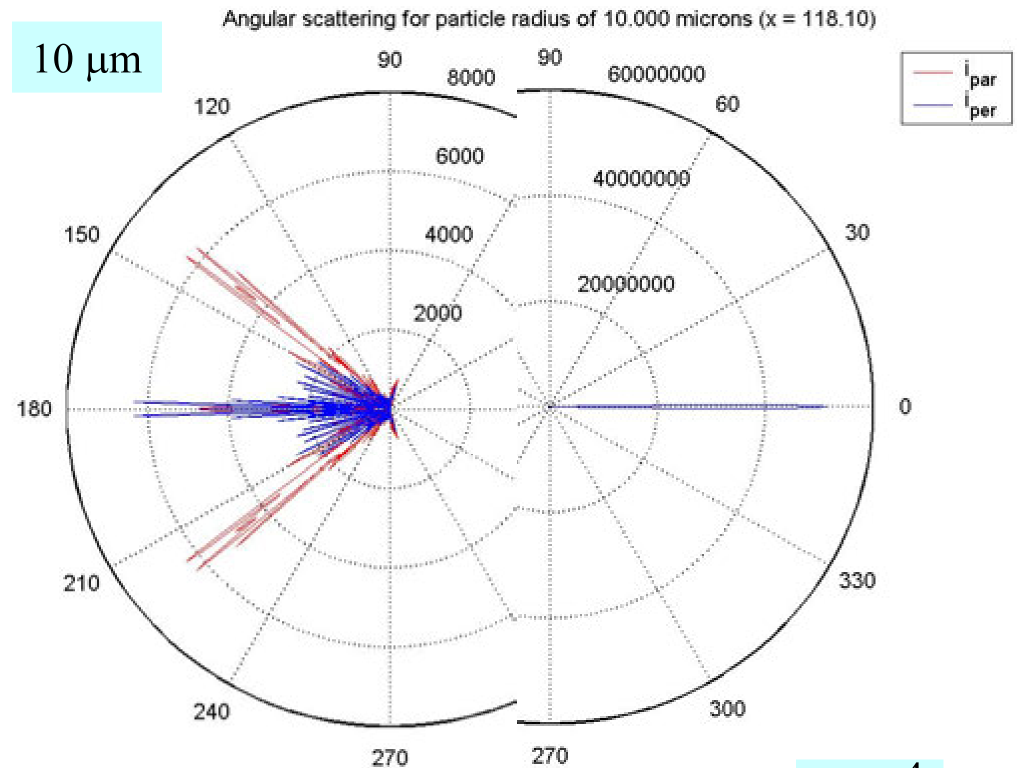

~x10^4

1 μm

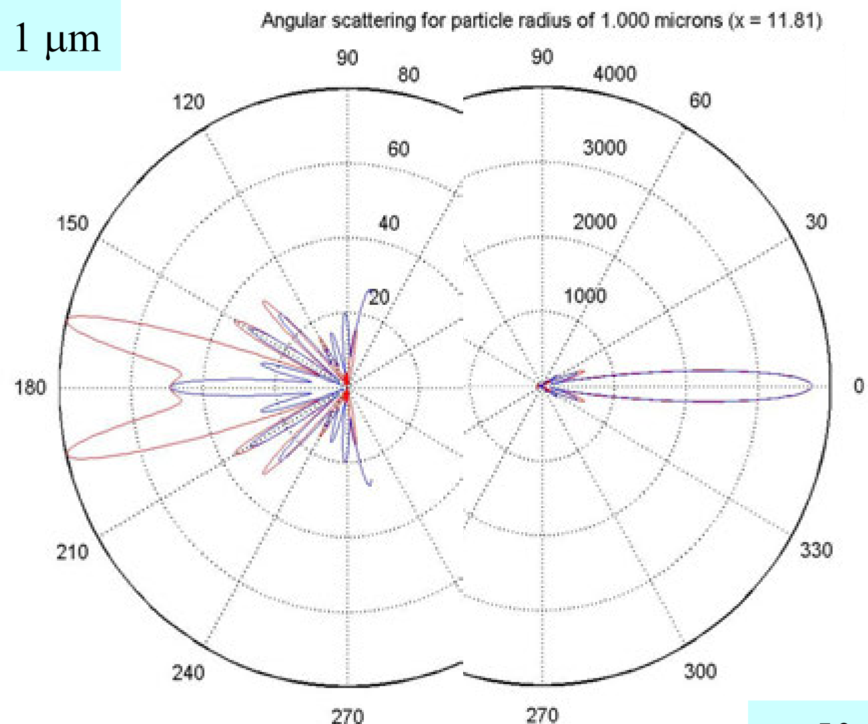

~x50

Backscatter –
Bistatic Lidar

Forward Lobe –
Aureole Laser

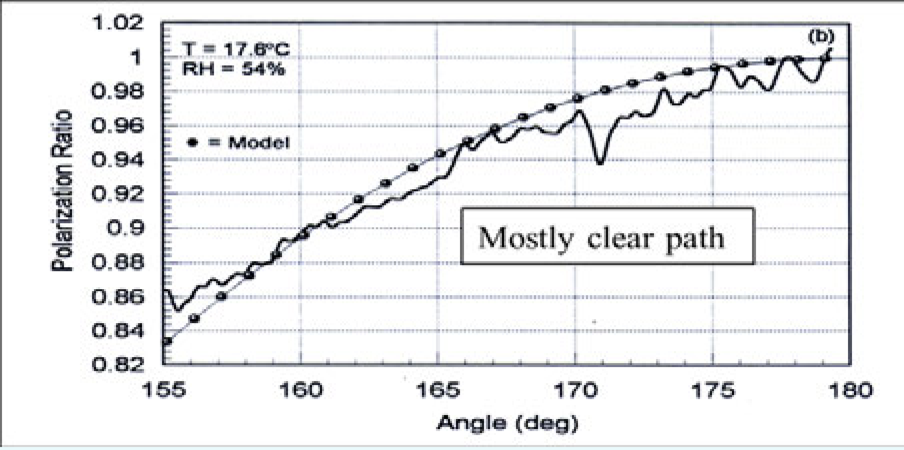

Polarization Ratio from Bistatic LIDAR

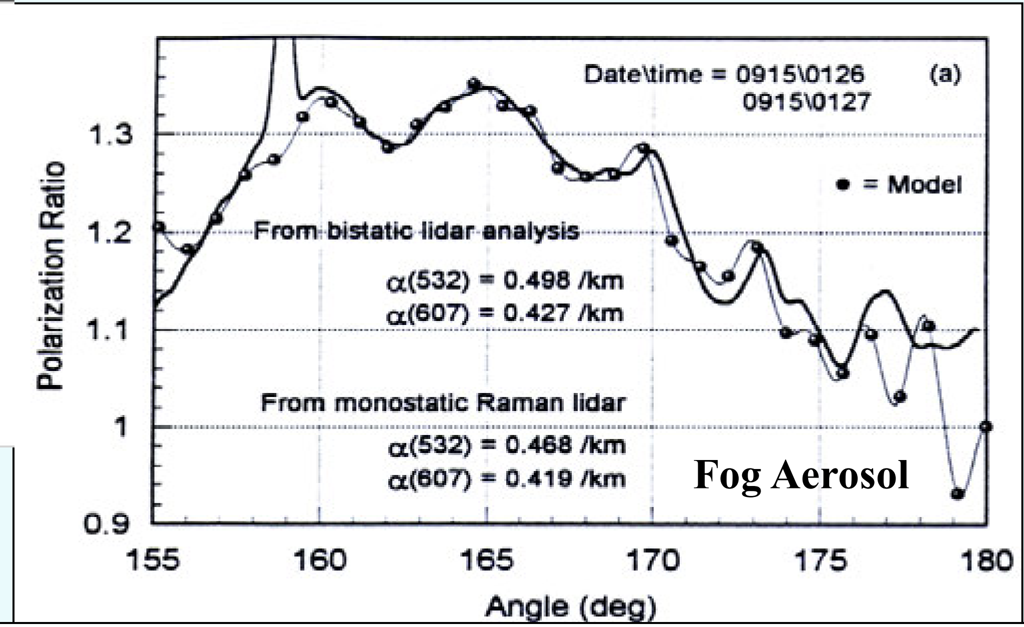

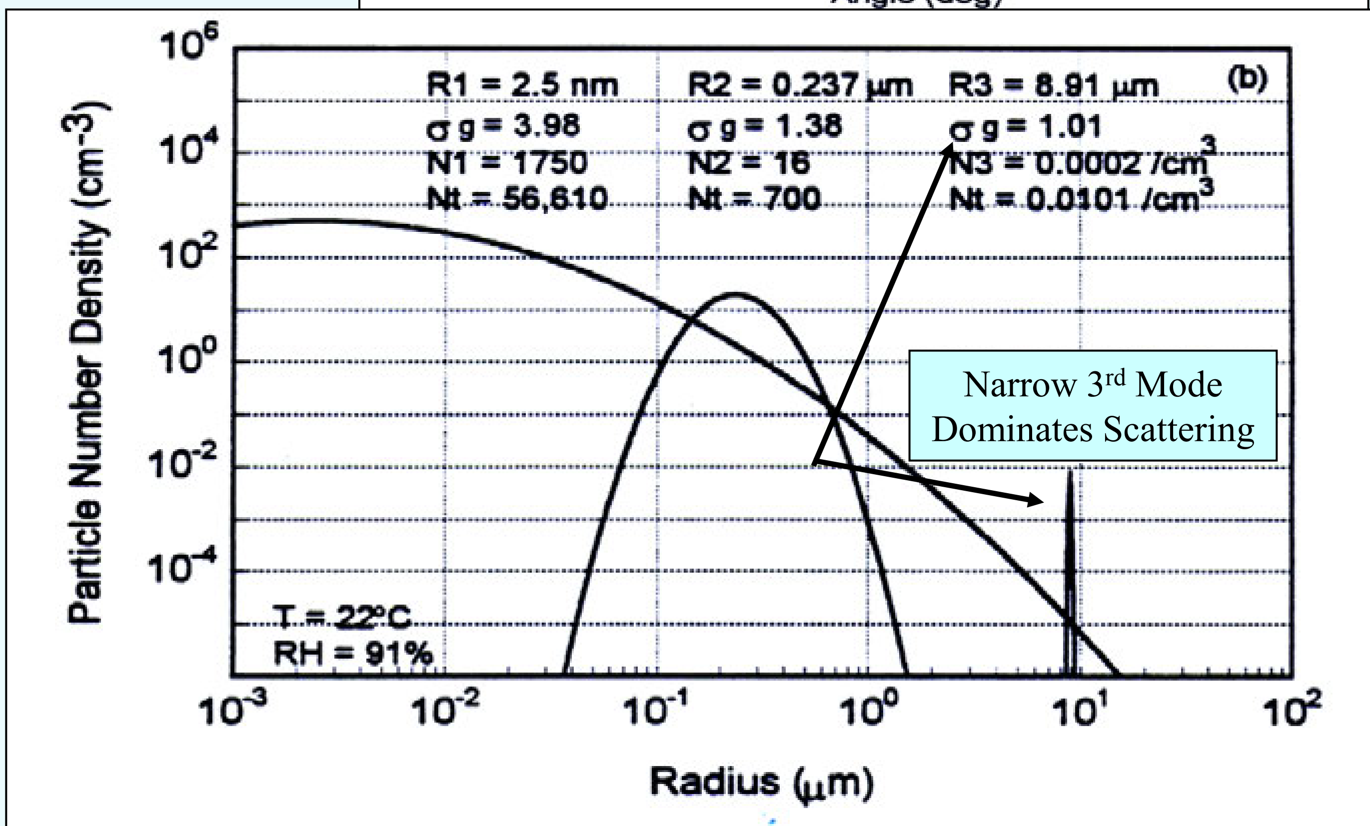

Polarization Ratio
Phase Functions

Backscatter (∥ ⊥)

Forward Scatter (∥ ⊥)

Trial 31 70 gm AzRD -- Polarization Ratio

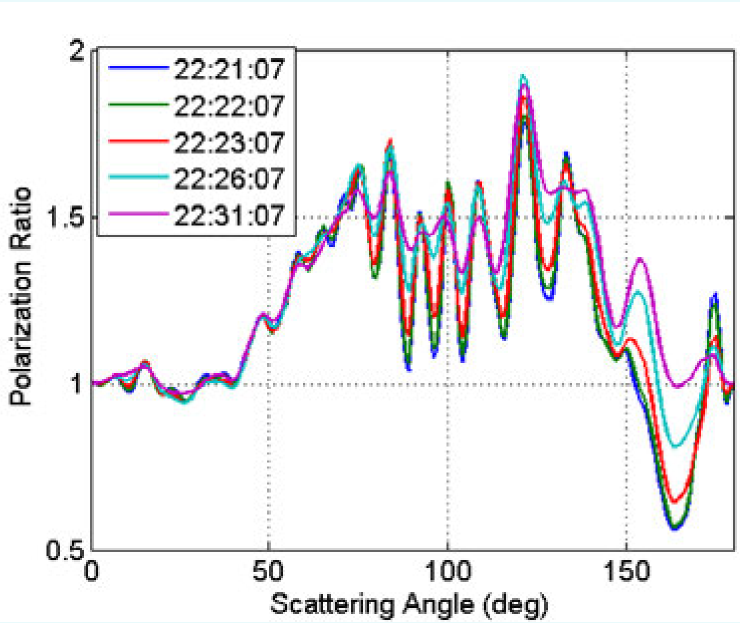

Trial 31 70 gm AzRD -- Backscatter Phase Functions

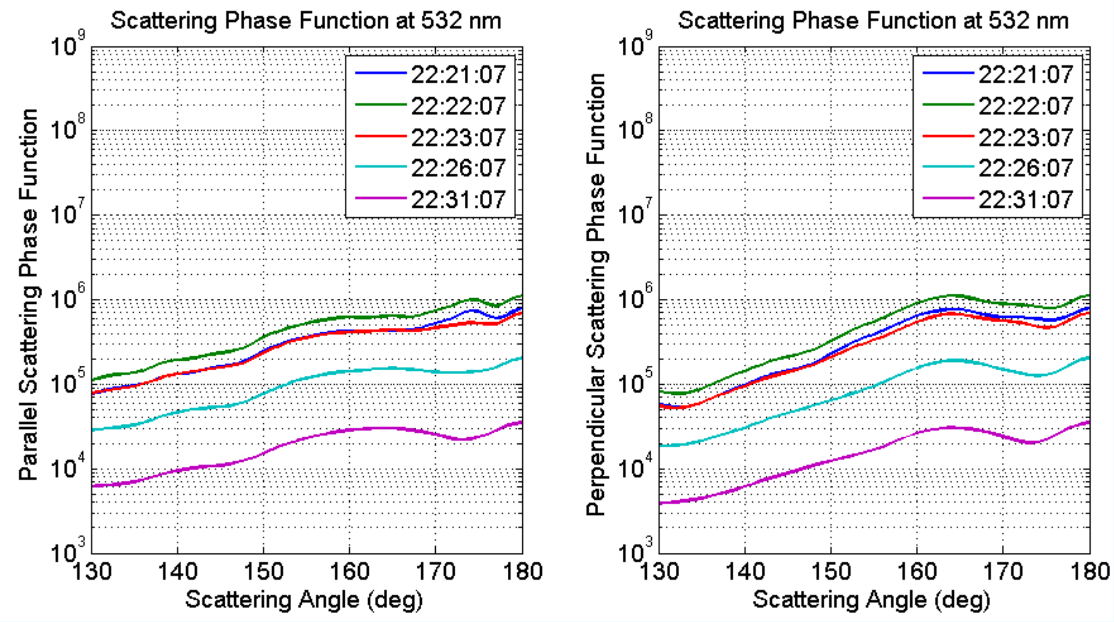

Trial 31 70 gm AzRD -- Forward Scatter Phase Functions

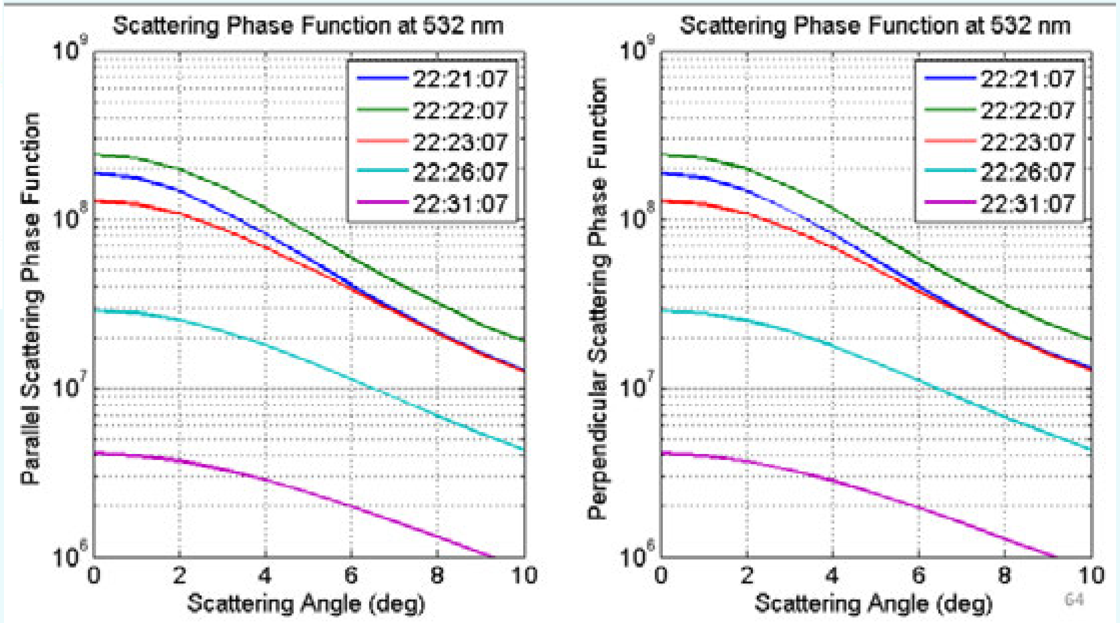

Laser Aureole

As the solar aureole provides a bulk measurement of the atmospheric aerosol haze, a laser aureole can be used to describe dust scatter.

Image on target board in Dust Chamber at 20m.

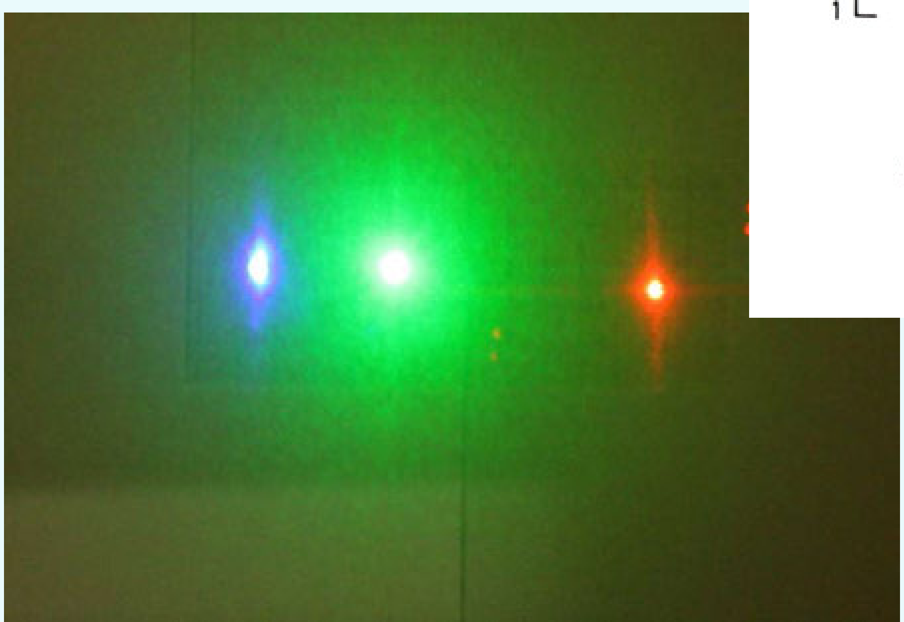

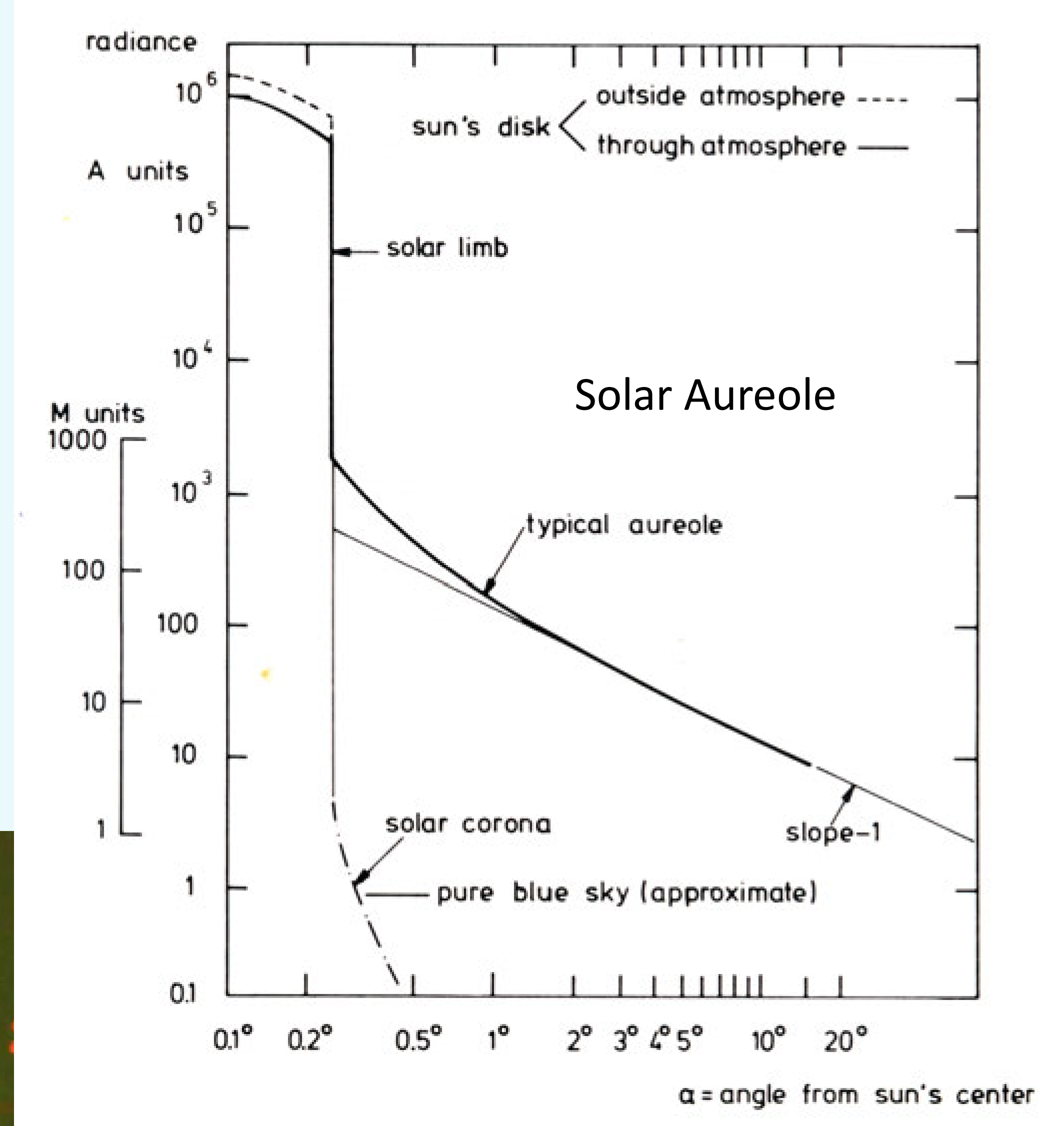

Secondary electron emission microscope images help characterize the size, shape, and chemical composition of dust aerosols. Useful measurements of the dust spectra may require special procedures to obtain the optical properties of thick aerosols, such as grinding the dust prior to making ellipsometry and spectroscopy measurements.

The optical scattering phase function, and the associated laser aureole, provide useful signatures that can describe the effective particle size distribution.

Summary & Status

Capabilities now demonstrated:

1. Single wavelength laser – Range to edges of aerosol, or cloud height
2. Raman Lidar – H_2O, T, Multi-wavelength extinction (estimate size) profiles, NIR,VIS,UV
3. DIAL/DAS Lidar – Multi-laser analysis using on-line and off-line signal return for species
4. OPO/OPA Laser – Tunable for differential analysis of chemicals, resonance Raman in UV
5. Supercontinuum Lidar – Path integrated chemical concentrations, MWIR, NIR, VIS, UV
6. Bi-static Lidar – Two detectors of a polarized laser beam, de-pol multi-scat
7. Phase Function Lidar – Detectors and different angles (forward/back) determine size

And

8. Lab SEM, ellipsometry and spectroscopy for n and k, crude lidar measurement of size distribution, and assumption of approximate spherical particles has been demonstrated to provide useful optical path extinction from scattering and absorption ----

However:

(1) Size distribution of the particles - often unknown and required for Mie calculations,
(2) Non-spherical particle shape negates assumptions for Mie calculation scheme,
(3) Dust materials with multiple types of chemical species, coatings on larger particles,
(4) Suspension, local wind and past weathering influence distribution, size, shape, type, and coatings of the particles

--- SO, A NUMBER OF APPROXIMATIONS ARE NEEDED IN THE COMPLEX CASES

Acknowledgments

The PSU lidar development, testing, and field investigations have been supported by the following organizations: supported by the following organizations: AFCRL (AFGL, AFRL), US Navy through SPAWAR PMW-185, NAVOCEANO, NAWC Point Mugu, ONR, DOE, EPA, Pennsylvania DEP, California ARB, NASA and NSF. The vision and backing of Carl Hoffman, Ed Harrison and Ed Mozley have been most valuable during this development. The hardware and software development has been possible because of the excellent efforts of several engineers and technicians at the PSU Applied Research Laboratory and the Department of Electrical Engineering. Special appreciation goes to D. Sipler, B. Dix, D.B. Lysak, T.M. Petach, F. Balsiger, T.D. Stevens, P.A.T. Haris, M. O'Brien, S.T. Esposito, K. Mulik, A. Achey, E. Novitsky, G. Li, D. Brown, A. Brown, A. Willitsford, A. Hook, G. Pangle, P. Edwards, and many additional graduate students who have made contributions to these efforts. The NE-OPS research investigations have been supported by the USEPA STAR Grants Program #R826373, Investigations of Factors Determining the Occurrence of Ozone and Fine Particles in Northeastern USA, and by the Pennsylvania DEP grant for the 2002 program. The efforts and cooperation of the several university investigators and government laboratory researchers is gratefully acknowledged. The effort and contributions of Rich Clark, S.T. Rao, George Allen, Bill Ryan, Bruce Doddridge, Steve McDow, Delbert Eatough, Susan Weirman and Fred Hauptman are particularly acknowledged because of their very significant contributions to the program.